



HAL
open science

Nuclear Receptor Subfamily 1 Group D Member 1 Regulates Circadian Activity Of NLRP3 Inflammasome to Reduce the Severity of Fulminant Hepatitis in Mice

Benoit Pourcet, Mathilde Zecchin, Lise Ferri, Justine Beauchamp, Sadichha Sitaula, C. Billon, Stéphanie Delhayé, Jonathan Vanhoutte, Alicia Mayeuf-Louchart, Quentin Thorel, et al.

► To cite this version:

Benoit Pourcet, Mathilde Zecchin, Lise Ferri, Justine Beauchamp, Sadichha Sitaula, et al.. Nuclear Receptor Subfamily 1 Group D Member 1 Regulates Circadian Activity Of NLRP3 Inflammasome to Reduce the Severity of Fulminant Hepatitis in Mice. *Gastroenterology*, 2018, *Gastroenterology*, 154 (5), pp.1449-1464. 10.1053/j.gastro.2017.12.019 . inserm-01701933

HAL Id: inserm-01701933

<https://inserm.hal.science/inserm-01701933>

Submitted on 13 Feb 2018

HAL is a multi-disciplinary open access archive for the deposit and dissemination of scientific research documents, whether they are published or not. The documents may come from teaching and research institutions in France or abroad, or from public or private research centers.

L'archive ouverte pluridisciplinaire **HAL**, est destinée au dépôt et à la diffusion de documents scientifiques de niveau recherche, publiés ou non, émanant des établissements d'enseignement et de recherche français ou étrangers, des laboratoires publics ou privés.

Nuclear Receptor Subfamily 1 Group D Member 1 Regulates Circadian Activity Of NLRP3 Inflammasome to Reduce the Severity of Fulminant Hepatitis in Mice

Author's names

Pourcet B^{1,3}, Zecchin M^{1,3}, Ferri L¹, Beauchamp J¹, Sitaula S², Billon C², Delhaye S¹, Vanhoutte J¹, Mayeuf-Louchart A¹, Thorel Q¹, Haas J¹, Eeckhoutte J¹, Dombrowicz D¹, Duhem C¹, Boulinguez A¹, Lancel S¹, Sebti Y¹, Burris T², Staels B¹ & Duez H^{1*}.

Author's institutions

¹European Genomic Institute for Diabetes (EGID), FR 3508, F-59000 Lille, France; Univ. Lille, F-59000 Lille, France; INSERM UMR 1011, F-59000 Lille, France; Institut Pasteur de Lille, F-59000 Lille, France.

²Department of Pharmacology and Physiology, Saint Louis University School of Medicine, St. Louis, MO, USA. The Scripps Research Institute, Jupiter, FL, USA.

³These authors contributed equally to this work

Corresponding author contact

*Correspondence should be addressed to H el ene Duez, UMR1011, Institut Pasteur de Lille, 1 rue Calmette, F-59019 Lille, France.

Tel: +33(0)3 2087 7793, email: helene.duez@pasteur-lille.fr

Author contributions

BP, MZ and HD conceived the project, designed and performed experiments, analysed the results and wrote the manuscript; LF and JB performed key experiments, analysed the results and read the manuscript; SS, CB and TPB designed and performed key experiments, analysed the results and read the manuscript; SD, JV, AML, QT, DD, CD, AB, YS, SL performed experiments and read the manuscript; JH performed cosinor analysis; JE analysed ChIPseq and 5'GROseq databases and read the manuscript; SD was in charge of the mouse colonies and read the manuscript; BS discussed the experiments and read the manuscript.

Acknowledgments

We thank Sami Lasri and Emmanuelle Vallez for their technical assistance. We also thank John Walker for overseeing the chemical synthesis of SR9009 and SR10067. We thank the BICeL Facility for access to systems and technical advice.

Conflict of interest statements

The authors disclose no conflicts

Fundings

This work was supported by research grants from R egion Nord Pas-de-Calais (to BP), Fondation pour la Recherche M edicale FRM (FDT20170739031) (to MZ), F ed eration Francophone de Recherche sur

le Diabète FFRD, sponsored by Fédération Française des Diabétiques (AFD), AstraZeneca, Eli Lilly, Merck Sharp & Dohme (MSD), Novo Nordisk & Sanofi, (to HD), Fondation de France (to HD), Région Nord-Pas-de-Calais (CPER) starting grant (to HD), the European Commission (FP7-HEALTH) consortium Eurhythdia (grant number 278397) (to BS and HD), the 'European Genomic Institute for Diabetes' (EGID, ANR-10-LABX-46) (to HD and BS), an unrestricted ITMO/Astra Zeneca grant (to BS), and from the American Heart Association (to SS; 14PRE1826000) and the National Institutes of Health (to TPB; MH093429).

Abbreviations used in this paper: ALAT, alanine aminotransferase; ASC, Apoptosis-associated Speck-like protein containing a Caspase recruitment domain protein; ATP, adenosine triphosphate; BMDMs, bone marrow-derived macrophages; CASP1, caspase-1; DAMPs, danger-associated molecular patterns; D-GalN, D-galactosamine; ELISA, enzyme-linked immunosorbent assay; FH, Fulminant Hepatitis; IL, interleukin; LPS, lipopolysaccharide; MDMs, monocyte-derived macrophages; NET, Neutrophil Extracellular Traps; NLRP3, NACHT, LRR, and pyrin domain-containing protein 3; PBS, phosphate-buffered saline; PECs, Peritoneum Exudate Cells; siRNA, small interfering RNA; ZT, zeitgeber.

Abstract

Background & Aims: The innate immune system responds not only to bacterial signals, but also to non-infectious danger-associated molecular patterns that activate the NLRP3 inflammasome complex after tissue injury. Immune functions vary over the course of the day, but it is not clear whether these changes affect the activity of the NLRP3 inflammasome. We investigated whether the core clock component nuclear receptor subfamily 1 group D member 1 (NR1D1, also called Rev-erba) regulates expression, activity of the NLRP3 inflammasome, and its signaling pathway.

Methods: We collected naïve peritoneal macrophages and plasma, at multiple times of day, from *Nr1d1*^{-/-} mice and their *Nr1d1*^{+/+} littermates (controls) and analyzed expression of NLR family pyrin domain containing 3 (NLRP3), interleukin 1 beta (IL1B, in plasma), and IL18 (in plasma). We also collected bone marrow-derived primary macrophages from these mice. Levels of NR1D1 were knocked down with small hairpin RNAs in human primary macrophages. Bone marrow-derived primary macrophages from mice and human primary macrophages were incubated with lipopolysaccharide (LPS) to induce expression of NLRP3, IL1B and IL18; cells were incubated with LPS and ATP to activate the NLRP3 complex. We analyzed caspase 1 activity and cytokine secretion. NR1D1 was activated in primary mouse and human macrophages by incubation with SR9009; some of the cells were also incubated with an NLRP3 inhibitor or inhibitors of caspase 1. *Nr1d1*^{-/-} mice and control mice were given intraperitoneal injections of LPS to induce peritoneal inflammation; plasma samples were isolated and levels of cytokines were

measured. *Nr1d1*^{-/-} mice, control mice, and control mice given injections of SR9009 were given LPS and galactosamine to induce fulminant hepatitis and MCC950 to specifically inhibit NLRP3; plasma was collected to measure cytokines and a marker of liver failure (ALAT); liver tissues were collected and analyzed by quantitative PCR, immunohistochemistry, and flow cytometry.

Results: In peritoneal macrophages, expression of NLRP3 and activation of its complex varied with time of day (circadian rhythm)—this regulation required NR1D1. Primary macrophages from *Nr1d1*^{-/-} mice and human macrophages with knockdown of NR1D1 had altered expression patterns of NLRP3, compared to macrophages that expressed NR1D1, and altered patterns of IL1B and 1L18 production. Mice with disruption of *Nr1d1* developed more-severe acute peritoneal inflammation and fulminant hepatitis than control mice. Incubation of macrophage with the NR1D1 activator SR9009 reduced expression of NLRP3 and secretion of cytokines. Mice given SR9009 developed less-severe liver failure and had longer survival times than mice given saline (control).

Conclusions: In studies of *Nr1d1*^{-/-} mice and human macrophages with pharmacologic activation of NR1D1, we found NR1D1 to regulate the timing of NLRP3 expression and production of inflammatory cytokines by macrophages. Activation of NR1D1 reduced the severity of peritoneal inflammation and fulminant hepatitis in mice.

KEY WORDS: immune regulation; biological clock; acute liver failure; rev-erb-alpha; DAMPs

Introduction

Fulminant hepatitis (FH) is a life-threatening pathological condition characterized by a fast evolving hepatic dysfunction associated with encephalopathy and coagulopathy¹. FH is triggered by numerous etiological factors such as viral infection, absorption of toxic compounds, metabolic and genetic diseases¹. However, the overdose of drugs such as acetaminophen is still the main cause of FH. Acetaminophen accumulation leads to P450-mediated overproduction of toxic metabolites provoking oxidative stress, mitochondrial membrane potential loss and hepatocellular death. This entrains the secretion of Danger-Associated Molecular Pattern (DAMPs) and activation of the innate immune system, leading to secretion of a large number of pro-inflammatory mediators¹. So far, no specific treatment is available apart from liver transplantation, pleading for an urgent need to identify pharmacological targets and to uncover the underlying mechanisms.

Organisms rely on a well-conserved molecular clockwork in order to anticipate changes imposed by the rotation of the Earth and gate physiological processes to the most appropriate time window². Immune functions vary according to the time-of-day, and clock disruption leads to inflammatory diseases³⁻⁵. Indeed, mounting evidences argue for the existence of a circadian rhythmicity in several immune functions including trafficking and abundance of blood leukocytes, and their recruitment to tissues^{3, 6-9}, although the underlying mechanisms are not elucidated yet. The importance of appropriate timing of the immune response is supported by the more severe response to endotoxin, *i.e.* increased macrophage cytokine production and increased mortality, upon clock dysfunction during chronic jetlag¹⁰.

The biological clock is a complex network of transcription factors and interlocked transcriptional feedback loops that orchestrate circadian rhythms of various physiological processes^{2, 3}. Clock dysfunction is associated with the development of metabolic and cardio-vascular disorders as well as cancers, and, as described above, immune defects, underscoring its central role in behaviour and physiology. Among the core clock components, the ligand-activated nuclear receptor and transcriptional repressor NR1D1 participates in the circadian control of hepatic glucose, lipid and bile acid metabolism¹¹⁻¹⁶, muscle mitochondrial activity¹⁷ and body temperature¹⁸. Lymphoid organs and immune cells such as macrophages harbour an intrinsic clockwork that drives circadian transcription of genes involved, for instance, in interleukin (IL) secretion and the Toll-like Receptor (TLR)-4 inflammatory pathway, leading to marked circadian variations in the response to endotoxin or bacterial challenge¹⁹⁻²¹. Interestingly, NR1D1 has previously been linked to the immune system as it represses *TLR4* and *Cx3cr1* expression in macrophages^{22, 23}. In addition, LPS-treated peritoneal macrophages from *Nr1d1*^{-/-} mice display increased *Ccl2* (*Mcp1*) expression, whereas pharmacological activation of NR1D1 represses the expression and release of IL-6²⁰.

The innate immune system recognizes and responds not only to bacterial components but also to non-infectious, structurally diverse DAMPs, such as crystals or extracellular ATP²⁴⁻²⁶, mounting an immune response to clear these factors²⁷. The NLRP3 inflammasome complex is central to this response and is activated by a two-step mechanism. *Nlrp3* gene expression is first primed by pro-inflammatory stimuli such as LPS or Neutrophil Extracellular Traps (NET)^{24, 26}. DAMPs then act as secondary signals to trigger several pathways activating the NLRP3 inflammasome including ATP-activated potassium efflux, translocation to mitochondria, reactive oxygen species production and release of mitochondrial DNA, cardiolipin and crystal-activated lysosomal cathepsins^{24, 25, 28-31}. Upon activation by infection or cellular

stresses, the NLRP3 inflammasome complex elicits the maturation of the pro-inflammatory cytokines IL1B and IL18³². Importantly, deregulation of NLRP3 participates in the development of IL18 and IL1B-driven auto-inflammatory diseases including atherosclerosis, gout and rheumatoid arthritis where accumulation of crystals of cholesterol, uric acid or hydroxyapatite is perceived as an endogenous sterile stress^{24, 33-36}, calling for therapeutic strategies to modulate inflammasome signaling. In addition, NLRP3 expression is increased in viral and drug-induced fulminant hepatitis, although its actual role in these pathological conditions is still underinvestigated^{37, 38}. Although the precise regulation of the NLRP3 inflammasome complex is of utmost importance in innate inflammation, whether it is controlled by the biological clock has not yet been demonstrated.

Here, we show that susceptibility to LPS/Galactosamine-induced fulminant hepatitis depends on the time of challenge in mice. Interestingly, we demonstrate that expression and activation of the NLRP3 inflammasome pathway oscillate in a daily manner under the direct control of NR1D1 in primary mouse and human macrophages. Macrophages from *Nr1d1*^{-/-} mice or human macrophages in which *Nr1d1* has been silenced mature and secrete higher amount of IL1B and IL18 in a NLRP3-dependent manner in response to DAMPs. The patho-physiological relevance of these observations has been tested *in vivo*. We demonstrate that the inflammasome is activated during peritonitis and acute hepatic liver failure. Furthermore, *NR1D1* deletion results in a higher NLRP3 inflammasome pathway activation, leading to exacerbated peritonitis and fulminant hepatitis, whereas pharmacological NR1D1 activation attenuates leucocyte infiltration, inflammasome activation, and liver injury thereby delaying death and improving the rate of survival from fulminant hepatitis. Collectively, these data identify NR1D1 as a pharmacological target for NLRP3-dependent inflammatory disorders and in particular in the context of acute fulminant hepatitis.

EXPERIMENTAL PROCEDURES

See the supplementary Materials and Methods section

Results

Diurnal variations in the rate and duration of survival after fulminant hepatitis induction

Fulminant hepatitis is an acute liver injury resulting from massive hepatocyte apoptosis, hemorrhagic necrosis and inflammation. Low doses of LPS in combination with the specific hepatotoxic agent D-

galactosamine (GalN) promote specific liver injury in mice and induce the production of inflammatory cytokines (TNF- α , IL1B and IL-6)³⁹ thus recapitulating the clinical picture of acute liver injury in humans³⁹. For these reasons, the LPS/GalN-induced hepatic injury is a widely used mouse model to understand fulminant hepatitis and its pharmacological treatment³⁹⁻⁴¹. Because the clock machinery controls the circadian behavior of the immune system, we hypothesized that the outcome of fulminant hepatitis may depend on the time of hepatitis induction. Mice were thus challenged with LPS/Galactosamine every 4 hours and their survival duration and rate was monitored for 48 hours. Strikingly, we demonstrate that death occurs after only 5 hours for all mice challenged with LPS/GalN at ZT16 while the survival duration of mice injected at ZT20 or ZT0 increases up to 8.5 hours with a survival rate reaching 40% (Figure 1A-B). Thus, mice display dramatic daily differences in their susceptibility to LPS/GalN-induced fulminant hepatitis, indicating a role of the circadian clock therein. We then searched for the oscillating pathways involved in these inflammatory processes³⁹⁻⁴².

The NLRP3 inflammasome pathway displays circadian rhythmicity

Because the NLRP3 inflammasome pathway is the central sensor of DAMPs released from necrotic tissues and may therefore play an essential role in fulminant hepatitis pathophysiology, we next determined whether *Nlrp3*, *Il1 β* and *Il18* gene expression as well as cytokine levels vary during the course of the day in macrophages isolated every 4 hours from the peritoneum of non-stimulated mice. Analysis of mRNA levels from CD11b⁺ peritoneal exudate cells (PECs) reveals that *Nlrp3*, *Il18*, *Il1 β* gene expression display strong daily variations with a minimum expression peak (nadir) at ZT4-8 and a maximum expression level (zenith) at ZT16-20 (Figure 1C-E and supplementary Figure 1). Accordingly, IL1B and IL18 secretion also shows cyclic variations *in vivo* (Figure 1F-G and Supplementary Figure 1). Accordingly, similar oscillations were observed in synchronized mouse bone marrow-derived macrophages (BMDM) (Supplementary Figure 2A-E and Supplementary Figure 1) and human monocyte-derived macrophages (hMDM) (Supplementary Figure 2F-J and Supplementary Figure 1).

NR1D1 governs circadian rhythmicity of the NLRP3 inflammasome pathway

Interestingly, *Nlrp3* gene expression is maximal at the time *Nr1d1* reaches a nadir (ZT20) (Figure 1C vs H, Supplementary Figure 1A vs D and Supplementary Figure 2F vs I). Thus, we wondered whether the rhythmicity observed in NLRP3 inflammasome expression and IL1B and IL18 expression and secretion

is under the direct control of NR1D1. Analysis of *Nr1d1*^{-/-} PECs and synchronized BMDM revealed an altered rhythmicity of *Nlrp3* expression compared to the one in *Nr1d1*^{+/+} PECs and synchronized BMDM (Figure 1C and Supplementary Figure 2D), demonstrating that NR1D1 is essential to drive circadian *Nlrp3* gene expression. Accordingly, oscillations in *Il1β* and *Il18* mRNA levels were blunted or phase-shifted in *Nr1d1*^{-/-} PECs and synchronized BMDM compared to *Nr1d1*^{+/+} cells (Figure 1D-E and Supplementary Figure 2E). *Bmal1* (*Arntl*) was measured as a control for NR1D1 activity (Supplementary Figure 2C, H). The secretion of IL1B and IL18, which is rhythmic in *Nr1d1*^{+/+} mice (Figure 1F-G), was found phase-delayed in *Nr1d1*^{-/-} mice. Collectively, our data demonstrate that NR1D1 drives circadian *Nlrp3* expression and ensuing rhythmic IL1B and IL18 secretion.

NR1D1 directly regulates Nlrp3 gene expression and activation in macrophages

NLRP3 expression is enhanced by exposure to pathogens and is activated by specific, structurally diverse molecular patterns associated to danger such as, for instance, extracellular ATP released by injured cells, the presence of microbial toxins including nigericin or accumulated crystals (eg cholesterol, alum)^{24, 25}. We thus investigated whether NR1D1 directly controls NLRP3 expression and activation in human MDMs and mouse primary bone marrow-derived macrophages (BMDMs) after LPS priming. *Nlrp3* mRNA levels were significantly higher in LPS-primed mouse and human macrophages in absence of *Nr1d1* (Figure 2A-B). Interestingly, analysis of ChIPseq and 5'GROseq data from RAW264.7 cells²³ indicated that NR1D1 occupies two sites located at -0.2 and -1.2 kb from the transcription start site (TSS), and inhibits *de novo* transcription from the -1.2 kb site (Supplementary Figure 3A). ChIP experiments showed that NR1D1 occupies these two sites also in wild-type BMDMs as well as two additional response elements at -4.4 and -4.2kb identified by *in silico* analysis (Figure 2C). Consistent with an active repression of these sites by NR1D1, we observed an increase of H3K27me3, a histone mark associated with a transcriptional repression⁴³, in wild-type compared to *Nr1d1*-deficient BMDMs (Figure 2D). Interestingly, the lack of a functional DNA binding domain in NR1D1 mimics the effect of *Nr1d1* deficiency on *Nlrp3* mRNA levels in LPS-treated BMDM (Figure 2E), thus emphasizing the importance of the direct binding of NR1D1 to DNA in this regulatory mechanism. Interestingly, 1 hour-LPS treatment strongly decreased NR1D1 binding to these sites, likely allowing a de-repression of the NLRP3 pathway in response to inflammatory stimuli, when a full response is needed to restore homeostasis (Figure 2C). Accordingly, short exposure to LPS increased *Nlrp3*, *Il1β* and *Il18* mRNA

expression but did not alter neither *Nr1d1* nor *Nr1d2* mRNA levels (Supplementary Figure 3B-F), thus suggesting that LPS priming triggers NR1D1 removal from its response elements without affecting its expression. However, prolonged exposure to LPS decreases *Nr1d1* and *Nr1d2* gene expression (Supplementary Figure 4A-B and Supplementary Figure 4E-F) but does not change their phase in synchronised BMDMs (data not shown). It is thus likely that both phenomena concur *in vivo*. In addition, Nlrp3 protein levels were higher in BMDMs from *Nr1d1*^{-/-} mice (Figure 2F and Supplementary Figure 3G-H). Upon activation by DAMPs, the NLRP3 protein associates with the Apoptosis-associated Speck-like protein containing a Caspase recruitment domain protein (ASC) to form ASC specks⁴⁴, a hallmark of cellular activation of the NLRP3 inflammasome. *Nr1d1*-deficiency led to a marked elevation of the number of cells displaying ASC specks upon ATP or nigericin activation (Figure 2G-H), indicating that NR1D1 regulates NLRP3 inflammasome complex formation. These findings implicate NR1D1 as a negative regulator of NLRP3 expression and activation *in vitro*. Furthermore, *NR1D2* knock-down did not affect *Nlrp3* mRNA levels in BMDM (Figure 2I and Supplementary Figure 4A-B), but enhanced *NLRP3* as well as *IL1β* and *IL18* expression in LPS-primed human MDMs (Supplementary Figure 4C-F) suggesting that the *Nr1d2* isotype is not involved in this process in mouse macrophages, but displays redundant, and not synergistic, activity with NR1D1 in human macrophages. Finally, *NR1D1* deletion did not affect other inflammasomes such as AIM2 (Supplementary Figure 5A), or AIM2-mediated IL1B and IL18 maturation and secretion in LPS-primed BMDM challenged with the AIM2 activator poly(dA:dT) (Supplementary Figure 5B-C).

NR1D1 controls NLRP3-dependent maturation and secretion of IL1B and IL18 in a Caspase-1-dependent manner

The NLRP3 inflammasome complex regulates IL18 and IL1B processing and secretion at the post-transcriptional level through the oligomerization and auto-cleavage of an inactive p45 pro-Caspase-1 precursor into active p20 and p10 Caspase-1 subunits responsible for the subsequent maturation of IL1B and IL18^{24, 25, 44}. *Nr1d1* deficiency did not affect *cas1* gene expression (Supplementary figure 6A) nor p45 protein amount (Figure 3A-B, Supplementary Figure 6B-C), but enhanced Caspase-1 maturation in LPS-primed BMDMs that were either unstimulated or ATP-stimulated to activate the NLRP3 inflammasome (Figure 3A and Supplementary Figure 6D). Consistently, *NR1D1* knockdown in human MDMs (Supplementary Figure 7A) and *NR1D1* deletion in BMDMs (Figure 3C and

supplementary Figure 7B) increased IL1B secretion after LPS priming and activation with ATP. Similarly, IL18 secretion in culture medium from activated macrophages was increased (Figure 3D and supplementary Figure 7C). In addition, NR1D1 activation by its natural ligand hemin¹⁶ decreased LPS-primed ATP-stimulated IL1B and IL18 secretion (Figure 3E-F and Supplementary Figure 8A) in BMDMs and human MDMs. Although IL1B and IL18 may be processed by other caspases such as Caspase-8 or Caspase-11^{44, 45}, the increase in IL1B and IL18 secretion in *Nr1d1*^{-/-} BMDMs is Caspase-1 and NLRP3-dependent, since it was abolished by Caspase-1 inhibition (Figure 3C-D and supplementary Figure 9A-B) and *Nlrp3* silencing (Figure 3G-H). Accordingly, addition of MCC950, a specific NLRP3 inhibitor⁴⁶, blunted the effect of NR1D1 activation by hemin on IL1B and IL18 secretion (Figure 3E-F). Altogether, these results demonstrate that NR1D1 regulates macrophage IL1B and IL18 maturation and secretion in a NLRP3-dependent manner *in vitro*.

NR1D1 also regulates Il1β and Il18 at the gene expression level

In addition to its role on NLRP3-dependent IL18 and IL1B maturation, we also assessed whether NR1D1 regulates *Il18* and *Il1β* expression at the transcriptional level in primary macrophages. *Nr1d1*-deficiency in BMDMs or siRNA-mediated *NR1D1* knockdown in human MDMs led to higher IL1B and IL18 mRNA and protein levels after LPS priming (Figure 4A-D and Supplementary Figure 9C). ChIPseq and 5'GRO-seq data analysis from NR1D1-overexpressing RAW264.7 macrophages²³ indicate that NR1D1 binds to the *Il1β* promoter and inhibits its *de novo* transcription (Supplementary Figure 10). ChIP-qPCR analysis demonstrated that endogenous NR1D1 binds to the *Il1β* promoter also in BMDMs, thus showing that NR1D1 directly regulates *Il1β* expression (Figure 4E). In addition, impairment of NR1D1 direct DNA binding enhances *Il1β* gene expression (Figure 4F), which, together with the ChIP experiment results, suggests that NR1D1 directly inhibits *Il1β* gene transcription. Finally, *NR1D2* knockdown did not affect *Il1β* gene expression in mouse macrophages (Figure 4G), but enhanced *Il1β* gene expression in human MDM (Supplementary Figure 4D) as well as IL1B and IL18 secretion (Supplementary Figure 4G-H). However, no synergistic effect with *Nr1d1*-deficiency was observed, highlighting the redundant role of NR1D2 in the regulation of this pathway.

Pharmacological activation of NR1D1 inhibits the NLRP3 inflammasome pathway

Since *Nr1d1*-deficiency enhances the NLRP3 inflammasome pathway, we hypothesized that ligand-mediated activation of NR1D1 inhibits NLRP3 expression and subsequent maturation of IL1B. Indeed, pharmacological activation of NR1D1 with SR9009¹⁵ down-regulated *Nlrp3* gene expression in LPS-primed BMDMs (Figure 5A) and lowered NLRP3 protein amount (Figure 5B, Supplementary Figure 8B). Similar effects were observed in SR9009- and hemin-stimulated human MDMs (Figure 5C and Supplementary Figure 8C). In addition, SR9009- and hemin-activation of NR1D1 decreased *Il1β* and *Il18* mRNA levels (Figure 5D-F, Supplementary Figure 8D-E), as well as IL1B and IL18 protein amount, maturation and secretion (Figures 3E-F, 5G-J) in BMDMs and human MDMs. Altogether, these results emphasize the pharmacological potential of NR1D1 to control the inflammasome and pro-inflammatory pathways in innate immune cells.

NR1D1 attenuates NLRP3-mediated inflammation in acute peritonitis

We next determined whether NR1D1 regulates the NLRP3 inflammasome *in vivo* in an acute model of sterile peritoneal inflammation. Mice were pre-treated or not with the NLRP3 inhibitor MCC950, and challenged by intraperitoneal administration of LPS and alum to specifically activate the NLRP3 signaling pathway⁴⁷. IL1B in the peritoneum and IL1B and IL18 plasma levels were higher in *Nr1d1*^{-/-} compared to *Nr1d1*^{+/+} mice, especially upon LPS-priming and alum activation of NLRP3 (Figure 6A-C). Remarkably, this effect was totally abolished in presence of MCC950 (Figure 6A-C).

In response to infection or injection of LPS, macrophage cytokine secretion displays a circadian pattern with a higher response toward the end of the light phase compared to ZT0^{8, 20}. Accordingly, IL1B and IL18 secretion displayed daily variations in peritoneal exudates isolated from mice intraperitoneally challenged with LPS every 6 hours (Figure 6D-E). Pharmacological activation of NR1D1 with SR10067 decreased IL1B and IL18 secretion in LPS-injected mice around the clock and reduced the time-of-day variations in LPS-stimulated cytokine secretion (Figure 6D-E) indicating that NR1D1 activation normalizes the daily fluctuations of the NLRP3 inflammasome pathway in conditions of an overstimulated inflammatory response. In addition, the higher IL1B secretion observed in LPS/Alum challenged *Nr1d1*^{-/-} mice sacrificed at ZT8 was completely blunted when the peritonitis was induced 12-hour apart in mice that were sacrificed at ZT20 (Figure 6F), *ie.* when NR1D1 is nearly absent (Figure 6G), consistent with the concept that NR1D1 regulates the NLRP3 inflammasome pathway in a circadian

manner. Altogether these data indicate that NR1D1 inhibits peritonitis through its action on the NLRP3 inflammasome *in vivo*.

NR1D1 prevents NLRP3-mediated fulminant hepatitis

Interestingly, the NLRP3 inflammasome is enhanced in MHV-3-induced viral fulminant hepatitis³⁷, and in LPS/GalN-induced acute liver failure³⁸. In addition, low doses of LPS in combination with GalN increase NLRP3 protein and Caspase1 activity^{38, 42}. Therefore, we tested whether NR1D1 may ameliorate acute liver failure using this experimental setting³⁹.

Strikingly, liver damage was strongly increased in LPS/GalN-injected *Nr1d1*^{-/-} mice compared to littermate controls, while NLRP3 inhibition by MCC950 treatment protected *Nr1d1*^{-/-} mice from liver failure (Figure 7A-B). *NR1D1* deletion induced hepatic *F4/80* and *Ccl2* gene expression suggesting enhanced macrophage infiltration (Figure 7C and Supplementary Figure 11A). Finally, the induction of caspase 1 activity (Figure 7D), liver *Nlrp3* and *Il1β* gene expression and IL1B secretion (Figure 7E-F, Supplementary Figure 11B) by LPS/GalN treatment, was further enhanced upon *Nr1d1*-deficiency. TNFα is enhanced in fulminant hepatitis and plays an important role in the regulation of innate inflammatory responses. We thus verified whether the TNFα pathway alters the *Nr1d1*-mediated regulation of the NLRP3 inflammasome pathway. As expected, hepatic *TNFα* gene expression was increased in LPS/GalN-challenged mice. However, it was not affected by *NR1D1* deletion (Supplementary Figure 11C). In addition, although TNFα treatment enhances *Il1β* and *Nlrp3* gene expression in BMDM, *Nr1d1*-deficiency did not affect the effect of TNFα on this pathway (Supplementary Figure 11D-E). We next assessed whether NR1D1 activation can inhibit fulminant hepatitis. As expected, control mice died 6.5 hours after LPS/GalN injection at ZT2 and ~90% were dead by 9 hours. Strikingly, SR9009-treated mice lived longer compared to vehicle-treated mice and the majority of mice survived from fulminant hepatitis (~70% survival rate of SR9009 pre-treated mice) (Figure 7G). The increased survival rate upon SR9009 treatment was associated with decreased LPS/GalN-induced hepatic hemorrhage (Supplementary Figure 11F). SR9009 pre-treatment strongly decreased the induction of ALAT, a marker of hepatic dysfunction, by LPS/GalN (Figure 7H) and improved liver appearance (Supplementary Figure 11G). In addition, SR9009 prevented the increase of hepatic *F4/80* (Figure 7I) and *Ccl2* (Supplementary Figure 11I) gene expression, Caspase 1 activity (Figure 7J), hepatic *Nlrp3* and *Il1β* gene expression (Figure 7K-L) and IL1B blood levels (Supplementary figure 11H)

after LPS/GalN injection. It is noteworthy that co-treatment with MCC950 and SR9009 resulted in similar, but not additive, effects on ALAT activity and inflammasome pathway gene expression compared to treatment with MCC950 or SR9009 alone, indicating that NLRP3 mediates the effect of NR1D1 on these parameters (Figure 7 and supplementary Figure 11). In addition, SR9009 treatment did not alter LPS/GalN-induced *Tnfa* gene expression in liver (Supplementary Figure 11J). Finally, SR9009, but not MCC950, decreased the total number of hepatic leucocytes recruited upon LPS/GalN injection (Supplementary Figure 12A). More precisely, we performed FACS analysis, which demonstrates that SR9009 impaired the recruitment of infiltrating monocytes and macrophages (Supplementary Figure 12B-E) as well as the hepatic recruitment of neutrophils (Supplementary Figure 12F-G). As expected, SR9009, but not MCC950, inhibited *Nlpr3*, *Il1 β* and *Il18* gene expression in hepatic F4/80⁺ cells isolated from LPS-GalN challenged mice (Supplementary Figure 12H-J). Our results indicate that NR1D1 activation improves mice survival during LPS/GalN-induced fulminant hepatitis by decreasing CCL2-mediated hepatic infiltration of innate immune cells and by inhibiting the activation of the NLRP3 inflammasome pathway.

Discussion

The nuclear receptors NR1D1 and NR1D2 are now considered as core components of the clock machinery. Indeed, *Nr1d1*-deficiency leads to a circadian period shortening by half-an-hour. Although this triggers a subtle activity phase shift compared to wild-type mice after one subjective day, this results in for a dramatic shift after a prolonged period^{12, 48}. Interestingly, whereas *NR1D2* deletion alone does not trigger any effect on the circadian activity in mice, the circadian activity of *Nr1d1*^{-/-}*Nr1d2*^{-/-} mice is abolished, emphasizing the redundant activity of both nuclear receptors in this context¹². Because their expression itself displays daily variations, NR1D1 and NR1D2 drive oscillatory expression of their target genes involved, for instance, in hepatic lipid synthesis and storage^{11, 12}, bile acid synthesis¹³ and thermogenesis¹⁸. In addition to its role in the control of metabolism, *Nr1d1*'s circadian pattern has also an important impact on the daily behavior of the immune system by controlling the circadian variations in cytokine expression such as MCP-1/CCL2 and IL-6 in mouse macrophages²⁰. We provide here new insights on the regulatory role of NR1D1 in circadian immunity in human and mouse primary macrophages.

Our results identify NR1D1 as a novel regulator of the NLRP3 inflammasome, driving circadian rhythmicity in its expression, activation, and ensuing IL1B and IL18 maturation and secretion (Supplementary Figure 13). We demonstrate that *NR1D1* deletion or silencing in primary mouse and human MDMs results in exacerbated NLRP3-dependent IL1B and IL18 production. Our results further show that NR1D1 attenuates NLRP3-driven inflammation *in vivo* in models of acute peritonitis and fulminant hepatitis and demonstrate that pharmacological NR1D1 activation reduces NLRP3 expression and IL1B and IL18 production by macrophages, presenting a promising strategy to treat NLRP3-dependent inflammatory diseases.

Compared to other inflammasomes, NLRP3 is activated by a plethora of signals of different biological origin such as bacterial, fungal and viral pathogens, pore-forming toxins, crystals, aggregates (β -amyloid) and DAMPs (ATP)²⁴. As such, NLRP3 is a key platform centralizing the detection of different signals to activate pro-inflammatory cytokine maturation and secretion. Because of this central role, a better understanding of the mechanisms that govern NLRP3 inflammasome activation is an important step toward the development of novel therapeutic strategies to combat over-activation of the immune system. Circadian regulation of immunity has been proposed as a mechanism to prepare the organism for a higher risk of tissue damage and infection during the active phase and as a process to anticipate the regeneration of the immune system during the resting phase³. Our data demonstrate for the first time that the molecular clock controls the NLRP3 inflammasome and subsequent cytokine responses in activated macrophages, hence supporting the idea that the circadian clock not only regulates oscillations in blood leucocyte trafficking⁷, but is also involved in the very first step of the immune response such as pro-inflammatory signal sensing.

The response to pro-inflammatory stimuli such as LPS depends on the time of pro-inflammatory challenge^{8, 20}. In line, our data demonstrate that FH severity depends on the induction time (Figure 1). Accordingly, treatment of mice at ZT8 leads to a more pronounced secretion of IL1B and IL18 than at ZT20 (Figure 6), which furthermore is inversely correlated with NR1D1 expression (Figure 1). Since the enhanced immune response at ZT10-ZT12 is also responsible for a higher risk of septic shock and death, a well-balanced circadian immunity appears to be essential to preserve immune homeostasis³. In this context, it is important that Nr1d1 activity can be modulated by small synthetic molecules⁴⁹. Here, we show that pharmacological activation of NR1D1 has the potential to restrain immune responses at specific times of the day (Figure 6).

IL1B secretion has been shown to oscillate diurnally with a peak during the onset of the active phase⁵⁰. Our data obtained on mouse peritoneum corroborate this finding (Figure 1G), and we additionally show that secretion of IL18, the other IL-1 family member matured by the NLRP3 inflammasome pathway, also displays daily fluctuations in macrophages isolated from the peritoneum (Figure 1F). According to our data obtained from synchronized isolated human and mouse macrophages, we suggest that these oscillations are mainly due to the internal clock machinery of macrophages themselves (Figure 1 and Supplementary Figures 1 and 2). It is noteworthy that despite the fact that *Il1 β* and *Il18* gene expression was not in phase at the transcriptional level (Figure 1D-E), IL1B and IL18 secretion oscillates with the same peaks and nadirs (Figure 1F-G), suggesting that the mere regulation of cytokine gene transcription is not sufficient to account for the daily fluctuations of cytokine levels and that an additional step, namely post-translational modifications and maturation, is required to modulate this circadian pattern. In our study, *Nlrp3* expression oscillates around the clock under the control of NR1D1, supporting the idea that NLRP3 circadian rhythmicity may account for the daily pattern of IL1B and IL18 secretion.

Although the priming of *Nlrp3* expression is known as a key step of the inflammatory response^{51, 52}, the transcriptional control of *Nlrp3* is poorly understood. Here, we demonstrate that *Nr1d1*-deficiency strongly alters *Nlrp3*, *Il1 β* and *Il18* expression in unstimulated, but also in LPS-challenged peritoneal macrophages and in injured livers from LPS/GalN-treated mice (Figure 1, Figure 7). In addition, NR1D1 controls NLRP3 complex assembly, Caspase-1 maturation of pro-IL1B and pro-IL18 and their secretion in response to NLRP3 priming and activation in both human and murine primary macrophages. Thus, NR1D1 acts through a two-pronged mechanism, acting at the transcriptional level to repress *Nlrp3*, *Il1 β* and *Il18* gene expression, and by modulating IL1B and IL18 protein maturation and secretion through the activation of the inflammasome complex and Caspase 1.

Aberrant activation of the NLRP3 inflammasome is implicated in the pathogenesis of numerous diseases including type 2 diabetes, atherosclerosis, gout, rheumatoid arthritis and kidney diseases^{24, 34, 36, 45}, some of which have also been linked to disruption of the clock³. Our study points to NR1D1 as a plausible link between a dysregulated clock and NLRP3-driven pathologies. Indeed, *NR1D1* deletion led to an exacerbated response to acute inflammation such as sterile peritonitis (Figure 6A-C) and drug-induced FH (Figure 7) for which no therapy other than liver transplantation is effective at improving patient survival. Current treatments for NLRP3-dependent diseases include IL-1-targeting strategies⁵³

and glyburide⁵⁴. We now show that Rev-erb activation protects against acute liver failure and improves the survival rate in a mouse model of FH (Figure 7, Supplementary Figure 11), identifying NR1D1 as a novel therapeutic target for the treatment of FH. It is noteworthy that, compared to MCC950 which inhibits NLRP3, NR1D1 targets not only the NLRP3 inflammasome, but also *Ccl2* expression (Supplementary Figure 12), macrophage infiltration (Figure 7, Supplementary Figure 12) and likely LPS signalling through TLR4 regulation²², and therefore may lead to a stronger efficiency compared to the mere inhibition of the NLRP3 pathway and IL-1 maturation by MCC950. In conclusion, NR1D1 represents an interesting target to control the DAMP-mediated NLRP3-dependent inflammatory process in a circadian manner.

SUPPLEMENTAL INFORMATION

Supplemental information includes Supplemental Experimental Procedures, one table and thirteen figures.

REFERENCES

1. Cardoso FS, Marcelino P, Bagulho L, et al. Acute liver failure: An up-to-date approach. *J Crit Care* 2017;39:25-30.
2. Bass J. Circadian topology of metabolism. *Nature* 2012;491:348-356.
3. Curtis AM, Bellet MM, Sassone-Corsi P, et al. Circadian clock proteins and immunity. *Immunity*. 2014;40:178-186.
4. Early JO, Curtis AM. Immunometabolism: Is it under the eye of the clock? *Semin Immunol* 2016.
5. Man K, Loudon A, Chawla A. Immunity around the clock. *Science* 2016;354:999-1003.
6. Gibbs J, Ince L, Matthews L, et al. An epithelial circadian clock controls pulmonary inflammation and glucocorticoid action. *Nat.Med.* 2014;20:919-926.
7. Mendez-Ferrer S, Lucas D, Battista M, et al. Haematopoietic stem cell release is regulated by circadian oscillations. *Nature* 2008;452:442-447.
8. Nguyen KD, Fentress SJ, Qiu Y, et al. Circadian gene *Bmal1* regulates diurnal oscillations of Ly6C(hi) inflammatory monocytes. *Science* 2013;341:1483-8.
9. **Scheiermann C, Kunisaki Y**, Lucas D, et al. Adrenergic nerves govern circadian leukocyte recruitment to tissues. *Immunity*. 2012;37:290-301.
10. Castanon-Cervantes O, Wu M, Ehlen JC, et al. Dysregulation of inflammatory responses by chronic circadian disruption. *J.Immunol.* 2010;185:5796-5805.
11. Bugge A, Feng D, Everett LJ, et al. Rev-erbalph and Rev-erbbeta coordinately protect the circadian clock and normal metabolic function. *Genes Dev.* 2012;26:657-667.
12. Cho H, Zhao X, Hatori M, et al. Regulation of circadian behaviour and metabolism by REV-ERB-alpha and REV-ERB-beta. *Nature* 2012;485:123-127.
13. Duez H, van der Veen JN, Duhem C, et al. Regulation of bile acid synthesis by the nuclear receptor Rev-erbalph. *Gastroenterology* 2008;135:689-698.
14. Raspe E, Duez H, Mansen A, et al. Identification of Rev-erbalph as a physiological repressor of apoC-III gene transcription. *J.Lipid Res.* 2002;43:2172-2179.
15. **Solt LA, Wang Y**, Banerjee S, et al. Regulation of circadian behaviour and metabolism by synthetic REV-ERB agonists. *Nature* 2012;485:62-68.

16. Yin L, Wu N, Curtin JC, et al. Rev-erbalpha, a heme sensor that coordinates metabolic and circadian pathways. *Science* 2007;318:1786-1789.
17. **Woldt E, Sebti Y**, Solt LA, et al. Rev-erb-alpha modulates skeletal muscle oxidative capacity by regulating mitochondrial biogenesis and autophagy. *Nat.Med.* 2013;19:1039-1046.
18. Gerhart-Hines Z, Feng D, Emmett MJ, et al. The nuclear receptor Rev-erbalpha controls circadian thermogenic plasticity. *Nature* 2013;503:410-413.
19. Bellet MM, Deriu E, Liu JZ, et al. Circadian clock regulates the host response to Salmonella. *Proc.Natl.Acad.Sci.U.S.A* 2013;110:9897-9902.
20. **Gibbs JE, Blaikley J**, Beesley S, et al. The nuclear receptor REV-ERBalpha mediates circadian regulation of innate immunity through selective regulation of inflammatory cytokines. *Proc.Natl.Acad.Sci.U.S.A* 2012;109:582-587.
21. **Keller M, Mazuch J**, Abraham U, et al. A circadian clock in macrophages controls inflammatory immune responses. *Proc.Natl.Acad.Sci.U.S.A* 2009;106:21407-21412.
22. Fontaine C, Rigamonti E, Pourcet B, et al. The nuclear receptor Rev-erbalpha is a liver X receptor (LXR) target gene driving a negative feedback loop on select LXR-induced pathways in human macrophages. *Mol.Endocrinol.* 2008;22:1797-1811.
23. Lam MT, Cho H, Lesch HP, et al. Rev-Erbs repress macrophage gene expression by inhibiting enhancer-directed transcription. *Nature* 2013;498:511-515.
24. Lamkanfi M, Dixit VM. Mechanisms and functions of inflammasomes. *Cell* 2014;157:1013-1022.
25. Schroder K, Tschopp J. The inflammasomes. *Cell* 2010;140:821-832.
26. Warnatsch A, Ioannou M, Wang Q, et al. Inflammation. Neutrophil extracellular traps license macrophages for cytokine production in atherosclerosis. *Science* 2015;349:316-20.
27. Naik E, Dixit VM. Modulation of inflammasome activity for the treatment of auto-inflammatory disorders. *J.Clin.Immunol.* 2010;30:485-490.
28. Munoz-Planillo R, Kuffa P, Martinez-Colon G, et al. K(+) efflux is the common trigger of NLRP3 inflammasome activation by bacterial toxins and particulate matter. *Immunity* 2013;38:1142-53.
29. Nakahira K, Haspel JA, Rathinam VA, et al. Autophagy proteins regulate innate immune responses by inhibiting the release of mitochondrial DNA mediated by the NALP3 inflammasome. *Nat Immunol* 2011;12:222-30.
30. Subramanian N, Natarajan K, Clatworthy MR, et al. The adaptor MAVS promotes NLRP3 mitochondrial localization and inflammasome activation. *Cell* 2013;153:348-61.
31. Zhou R, Yazdi AS, Menu P, et al. A role for mitochondria in NLRP3 inflammasome activation. *Nature* 2011;469:221-5.
32. Latz E, Xiao TS, Stutz A. Activation and regulation of the inflammasomes. *Nat.Rev.Immunol.* 2013;13:397-411.
33. **Duewell P, Kono H**, Rayner KJ, et al. NLRP3 inflammasomes are required for atherogenesis and activated by cholesterol crystals. *Nature* 2010;464:1357-1361.
34. Masters SL, Latz E, O'Neill LA. The inflammasome in atherosclerosis and type 2 diabetes. *Sci.Transl.Med.* 2011;3:81ps17.
35. Sheedy FJ, Grebe A, Rayner KJ, et al. CD36 coordinates NLRP3 inflammasome activation by facilitating intracellular nucleation of soluble ligands into particulate ligands in sterile inflammation. *Nat.Immunol.* 2013;14:812-820.
36. Vande Walle L, Van Opdenbosch N, Jacques P, et al. Negative regulation of the NLRP3 inflammasome by A20 protects against arthritis. *Nature* 2014;512:69-73.
37. **Guo S, Yang C**, Diao B, et al. The NLRP3 Inflammasome and IL-1beta Accelerate Immunologically Mediated Pathology in Experimental Viral Fulminant Hepatitis. *PLoS Pathog* 2015;11:e1005155.
38. Seo MJ, Hong JM, Kim SJ, et al. Genipin protects d-galactosamine and lipopolysaccharide-induced hepatic injury through suppression of the necroptosis-mediated inflammasome signaling. *Eur J Pharmacol* 2017;812:128-137.
39. Furuya S, Kono H, Hara M, et al. Interleukin 17A plays a role in lipopolysaccharide/D-galactosamine-induced fulminant hepatic injury in mice. *J Surg Res* 2015;199:487-93.
40. Nakama T, Hirono S, Moriuchi A, et al. Etoposide prevents apoptosis in mouse liver with D-galactosamine/lipopolysaccharide-induced fulminant hepatic failure resulting in reduction of lethality. *Hepatology* 2001;33:1441-50.
41. Shirozu K, Hirai S, Tanaka T, et al. Farnesyltransferase inhibitor, tipifarnib, prevents galactosamine/lipopolysaccharide-induced acute liver failure. *Shock* 2014;42:570-7.
42. Zhong Z, Umemura A, Sanchez-Lopez E, et al. NF-kappaB Restricts Inflammasome Activation via Elimination of Damaged Mitochondria. *Cell* 2016;164:896-910.

43. **Zhang T, Cooper S**, Brockdorff N. The interplay of histone modifications - writers that read. *EMBO Rep* 2015;16:1467-81.
44. Broderick L, De Nardo D, Franklin BS, et al. The inflammasomes and autoinflammatory syndromes. *Annu.Rev.Pathol.* 2015;10:395-424.
45. **Guo H, Callaway JB**, Ting JP. Inflammasomes: mechanism of action, role in disease, and therapeutics. *Nat.Med.* 2015;21:677-687.
46. Coll RC, Robertson AA, Chae JJ, et al. A small-molecule inhibitor of the NLRP3 inflammasome for the treatment of inflammatory diseases. *Nat.Med.* 2015;21:248-255.
47. Guarda G, Braun M, Staehli F, et al. Type I interferon inhibits interleukin-1 production and inflammasome activation. *Immunity* 2011;34:213-23.
48. Preitner N, Damiola F, Lopez-Molina L, et al. The orphan nuclear receptor REV-ERB α controls circadian transcription within the positive limb of the mammalian circadian oscillator. *Cell* 2002;110:251-60.
49. Kojetin DJ, Burris TP. REV-ERB and ROR nuclear receptors as drug targets. *Nat Rev Drug Discov* 2014;13:197-216.
50. **Sherman H, Frumin I**, Gutman R, et al. Long-term restricted feeding alters circadian expression and reduces the level of inflammatory and disease markers. *J Cell Mol Med* 2011;15:2745-59.
51. Bauernfeind FG, Horvath G, Stutz A, et al. Cutting edge: NF-kappaB activating pattern recognition and cytokine receptors license NLRP3 inflammasome activation by regulating NLRP3 expression. *J Immunol* 2009;183:787-91.
52. Franchi L, Eigenbrod T, Nunez G. Cutting edge: TNF-alpha mediates sensitization to ATP and silica via the NLRP3 inflammasome in the absence of microbial stimulation. *J Immunol* 2009;183:792-6.
53. Dinarello CA, Simon A, van der Meer JW. Treating inflammation by blocking interleukin-1 in a broad spectrum of diseases. *Nat.Rev.Drug Discov.* 2012;11:633-652.
54. Lamkanfi M, Mueller JL, Vitari AC, et al. Glyburide inhibits the Cryopyrin/Nalp3 inflammasome. *J.Cell Biol.* 2009;187:61-70.

Author names in bold designate shared co-first authorship

FIGURE LEGENDS

Figure 1: NR1D1 controls daily variations in *Nlrp3* expression and activation, and IL1B and IL18 secretion.

(A) Survival time and (B) Survival rate after FH induction every for 4 hours. Data are means \pm SEM (n=4). ***p<0.001 as determined by Log-rank Mantel Cox (A) and Log-rank (B) test. (C) *Nlrp3*, (D) *Il18*, (E) *Il1 β* and (H) *Nr1d1* mRNA levels in CD11b⁺ PECs from unstimulated *Nr1d1*^{+/+} or *Nr1d1*^{-/-} mice obtained by peritoneal lavage around the clock (ZT4 \rightarrow ZT4). (F) Secreted IL18 and (G) IL1B in peritoneal lavages from unstimulated *Nr1d1*^{+/+} or *Nr1d1*^{-/-} mice around the clock (ZT4 \rightarrow ZT4). Data are means \pm SEM (n=4-7). *p<0.05, **p<0.01, ***p<0.001 as determined by two-way ANOVA and Bonferroni post-hoc test to compare *Nr1d1*^{+/+} and *Nr1d1*^{-/-}. ρ <0.05, ρ° <0.01, $\rho^{\circ\circ}$ <0.001 as determined by one-way ANOVA test to compare *Nr1d1*^{+/+}. \$p<0.05, \$\$p<0.01, \$\$\$p<0.001 as determined by one-way ANOVA test to compare *Nr1d1*^{-/-}. Cosinor analysis is given in Supplementary Figure 1. ZT0: lights on, ZT12: lights off.

Figure 2: NR1D1 directly regulates the NLRP3 inflammasome in macrophages.

Nlrp3 mRNA levels in control (CTRL) and LPS-primed (LPS) (A) BMDMs from *Nr1d1*^{+/+} and *Nr1d1*^{-/-} mice and in (B) MDMs transfected with siRNA against *Nr1d1* (siNr1d1) or a scrambled siRNA (siCTRL) (n=3). Data are represented as means ± SD. ***p<0.001 as determined by two-way ANOVA followed by a Bonferroni post-hoc test. (C) ChIP analysis of NR1D1 occupancy to the *Nlrp3* promoter in control (Vehicle) or LPS-primed (for 1 hour) BMDMs. The top diagram represents putative Rev-erb Response Elements (RevREs) unveiled by MatInspector promoter analysis. Down, ChIP analysis from one representative experiment. (D) ChIP analysis of H3K27me3 at the *Nlrp3* promoter in *Nr1d1*^{+/+} and *Nr1d1*^{-/-} BMDMs. (E) *Nlrp3* mRNA levels in BMDMs from *Nr1d1*^{Floxed/Floxed};LysM^{+/+} (*Nr1d1*^{Floxed/Floxed}) or *Nr1d1*^{Floxed/Floxed};LysM^{Cre/+} (*Nr1d1*^{DBDmut}) mice mice. (F) NLRP3 protein expression in control (CTRL) and LPS-primed ATP-activated (LPS ATP) BMDMs from *Nr1d1*^{+/+} or *Nr1d1*^{-/-} mice (n=3). Top, the western blot and down, its quantification. ***p<0.001 as determined by two-way ANOVA followed by a Bonferroni post-hoc test. (G) ASC specks formation and (H) its quantification in LPS-primed BMDMs from *Nr1d1*^{+/+} and *Nr1d1*^{-/-} mice treated with ATP, Nigericin or vehicle (CTRL). Results are presented as mean percentage of cells displaying ASC specks ± SD. *p<0.05, ***p<0.001 as determined by two-way ANOVA followed by a Bonferroni post-hoc test. (I) *Nlrp3* mRNA levels in BMDMs from *Nr1d1*^{+/+} and *Nr1d1*^{-/-} mice transfected with siRNA against *Nr1d2* (siNr1d2) or a scrambled siRNA (siCtrl) (n=3). Data are represented as means ± SD. ***p<0.001 as determined by two-way ANOVA followed by a Bonferroni post-hoc test.

Figure 3: NR1D1 regulates IL18 and IL1B maturation and secretion in a NLRP3 inflammasome-dependent manner.

Caspase-1 protein (sub-unit p10, p20, p35, p45) expression in supernatant (A) or lysate (B) from LPS-primed (LPS) and ATP-activated (LPS/ATP) or not (I) BMDMs from *Nr1d1*^{+/+} (*Rα*^{+/+}) and *Nr1d1*^{-/-} (*Rα*^{-/-}) mice (representative of 3 independent experiments). (C) IL1B and (D) IL18 secreted by LPS-primed and ATP-activated BMDMs isolated from *Nr1d1*^{+/+} or *Nr1d1*^{-/-} mice that were treated with low dose of caspase inhibitor z-VAD-fmk (z-VAD-fmk) or not (Vehicle) (n=3). (E) IL1B secreted by LPS-primed and ATP activated (ATP) or not (CTRL) BMDMs treated with (hemin) or its vehicle (vehicle) and with NLRP3 inhibitor MCC950 or not (Saline) (n=3). (F) IL18 secreted by LPS-primed and ATP-activated (ATP) or not (CTRL) MDMs treated with (hemin) or its vehicle (vehicle) and with NLRP3 inhibitor MCC950 or not

(Saline) (n=3). (G) IL1B and (H) IL18 secreted by LPS-primed and ATP-activated BMDMs isolated from *Nr1d1^{+/+}* or *Nr1d1^{-/-}* mice in which NLRP3 was silenced (siRNA NLRP3) or not (siRNA CTRL) (n=3). The top western blot (G) shows NLRP3 protein silencing. Data are represented as means \pm SD. ***p<0.001 as determined by two-way ANOVA followed by a Bonferroni post-hoc test.

Figure 4: NR1D1 regulates IL18 and IL1B expression.

(A-D) *Il18* (A,B) and *Il1 β* (C,D) mRNA levels in LPS-primed BMDMs isolated from *Nr1d1^{+/+}* or *Nr1d1^{-/-}* mice (A,C) and in LPS-primed human MDMs transfected with siRNA against *Nr1d1* (siNr1d1) or a scrambled siRNA (siCTRL) (B,D) (n=3). Data are represented as means \pm SD. **p<0.01, ***p<0.001 as determined by two-way ANOVA followed by a Bonferroni post-hoc test. (E) ChIP analysis of NR1D1 occupancy at the *Il1 β* and *Arntl* promoter (as control) in control (Vehicle) or LPS-primed (for 1 hour) BMDMs (n=3). The top diagram represents putative Rev-erb Response Elements (RevREs) unveiled by MatInspector promoter analysis. Data are represented as means \pm SD. **p<0.01, ***p<0.001 as determined by an unpaired t-test. *Il1 β* mRNA levels in LPS-primed (F) BMDMs isolated from *Nr1d1^{Floxed/Floxed};LysM^{+/+}* (*Nr1d1^{Floxed/Floxed}*) or *Nr1d1^{Floxed/Floxed};LysM^{Cre/+}* (*Nr1d1^{DBDmut}*) mice mice and (G) BMDMs from *Nr1d1^{+/+}* and *Nr1d1^{-/-}* mice transfected with siRNA against *Nr1d2* (siNr1d2) or a scrambled siRNA (siCtrl) (n=3). Data are represented as means \pm SD. ***p<0.001 as determined by two-way ANOVA followed by a Bonferroni post-hoc test.

Figure 5: NR1D1 pharmacological activation inhibits the NLRP3 inflammasome pathway in primary macrophages.

(A) *Nlrp3* mRNA levels in LPS-primed (LPS) or not (NT) BMDMs treated with SR9009 (n=3). (B) NLRP3 protein levels in LPS-primed (LPS) or not (V) BMDMs treated with SR9009 or DMSO (representative of 3 independent experiments). (C) *NLRP3* and (E) *IL1 β* mRNA levels in LPS-primed human MDMs pre-treated with SR9009 or not (Vehicle) (n=3). (D) *Il1 β* and (F) *Il18* mRNA levels in LPS-primed BMDMs pre-treated or not with SR9009 (n=3). (G) pro- and matured IL1B protein expression in LPS-primed BMDM or not (NT) and treated with SR9009 or not (Vhc). (H) IL1B secretion in LPS-primed and ATP-activated BMDMs pre-treated with SR9009 or not (Vehicle) (n=3) (I) IL1B and (J) IL18 secretion in LPS-primed and ATP-activated human MDMs pre-treated with SR9009 or not (Vehicle) (n=3). Data are represented as means \pm SD. ∞ p<0.001 in LPS vs unstimulated vehicle condition (A); *p<0.05, **p<0.01,

*** $p < 0.001$ as determined by one-way ANOVA (A) or two-way ANOVA (C-F, H-J) followed by a Bonferroni post-hoc test.

Figure 6: NR1D1 modulates the development of acute innate inflammation through regulation of the NLRP3 inflammasome in a peritonitis model.

(A) Secreted IL1B from peritoneal lavage of *Nr1d1^{+/+}* or *Nr1d1^{-/-}* mice treated with LPS, LPS + Alum, LPS + Alum + MCC950 or not (Ctrl) at ZT8 (n=6-12). (B) Plasma IL1B and (C) IL18 from *Nr1d1^{+/+}* or *Nr1d1^{-/-}* mice treated as in (A) (n=6-12). (D) Secreted IL1B and (E) IL18 from peritoneal macrophages isolated around the clock from LPS-stimulated mice treated with SR10067 (Ligand) or vehicle (n=10). (F) Secreted IL1B from peritoneal lavage at ZT8 and ZT20 of *Nr1d1^{+/+}* or *Nr1d1^{-/-}* mice treated with LPS + Alum (n=6-12). Data are represented as means \pm SEM. * $p < 0.05$, ** $p < 0.01$, *** $p < 0.001$ as determined by two-way ANOVA and Bonferroni post-hoc test. (G) NR1D1 protein expression in CD11b⁺ PECs at ZT8 and ZT20 of *Nr1d1^{+/+}* ($R\alpha^{+/+}$) or *Nr1d1^{-/-}* ($R\alpha^{-/-}$) mice treated with LPS + Alum (n=6-12).

Figure 7: NR1D1 prevents the development of fulminant hepatitis through regulation of the NLRP3 inflammasome.

(A-F) *Nr1d1^{+/+}* or *Nr1d1^{-/-}* mice were pre-treated with MCC950 or Saline and then intraperitoneally injected with LPS plus GalN or PBS as control (Ctrl). (A) Representative liver appearance, (B) serum ALAT activity, (C) liver *F4/80* mRNA levels, (D) Caspase-1 activity in tissue sections (FMI: Fluorescence Mean Intensity) and (E) *Nlrp3* and (F) *Il1 β* mRNA levels in liver from each group as described. Data are represented as means \pm SEM (n=5-11). * $p < 0.05$, ** $p < 0.01$, *** $p < 0.001$ as determined by two-way ANOVA and Bonferroni post-hoc test. (G-L) C57/Bl6 mice were pre-treated with SR9009 or vehicle and/or MCC950 and then challenged with LPS/GalN or PBS as control (Ctrl) as indicated. (G) Kaplan-Meier survival curve of mice challenged with LPS/GalN at ZT2 (n=15 per group). *** $p < 0.0001$ as determined by log rank test. (H) serum ALAT activity, (I) liver *F4/80* mRNA levels, (J) Caspase 1 activity in tissue sections (FMI: Fluorescence Mean Intensity), and (K) *Nlrp3* and (L) *Il1 β* mRNA levels in liver from each group as described. Data are represented as means \pm SEM (n=5-6) ** $p < 0.01$, *** $p < 0.001$ as determined by two-way ANOVA and Bonferroni post-hoc test.

Nuclear Receptor Subfamily 1 Group D Member 1 Regulates Circadian Activity of NLRP3 Inflammasome to Reduce the Severity of Fulminant Hepatitis in Mice

Author's names

Pourcet B^{1,3}, Zecchin M^{1,3}, Ferri L¹, Beauchamp J¹, Sitaula S², Billon C², Delhaye S¹, Vanhoutte J¹, Mayeuf-Louchart A¹, Thorel Q¹, Haas J¹, Eeckhoutte J¹, Dombrowicz D¹, Duhem C¹, Boulinguez A¹, Lancel S¹, Sebti Y¹, Burris T², Staels B¹ & Duez H^{1*}.

Author's institutions

¹European Genomic Institute for Diabetes (EGID), FR 3508, F-59000 Lille, France; Univ. Lille, F-59000 Lille, France; INSERM UMR 1011, F-59000 Lille, France; Institut Pasteur de Lille, F-59000 Lille, France.

²Department of Pharmacology and Physiology, Saint Louis University School of Medicine, St. Louis, MO, USA. The Scripps Research Institute, Jupiter, FL, USA.

³These authors contributed equally to this work

Corresponding author contact

*Correspondence should be addressed to H el ene Duez, UMR1011, Institut Pasteur de Lille, 1 rue Calmette, F-59019 Lille, France.

Tel: +33(0)3 2087 7793, email: helene.duez@pasteur-lille.fr

SUPPLEMENTARY MATERIAL

SUPPLEMENTAL EXPERIMENTAL PROCEDURES

Mice

The wild-type C57/Bl6 8-week old female mice used for pharmacological investigations were purchased from Charles River (Orl ans, France). *Nr1d1*^{-/-} mice were obtained from B. Vennstr om and backcrossed for 8 generations with sv129 mice. *Nr1d1*^{DBDmut} floxed mice were obtained from the Institut Clinique de la Souris (Illkirch, France) and characterized elsewhere¹. Myeloid-specific *Nr1d1*^{DBDmut} mice were generated by breeding C57/Bl6 *Nr1d1*^{DBDmut fl/fl} mice with *LysM*^{Cre/+} mice from the Jackson laboratory (<https://www.jax.org/>). Mice were housed in a 12:12- light/dark cycle and fed a chow diet *ad libitum*. All animal procedures conducted at Lille were approved by the local ethics committee (CEEA75). Mouse experimentation performed in wild-type mice at Saint Louis University were approved by the SLU IACUC.

Circadian rhythm

Nr1d1^{-/-} and *Nr1d1*^{+/+} mice were sacrificed around the clock every 4 hours (ZT0 light on, ZT4, ZT8, ZT12 light off, ZT16, ZT20 and ZT24). Peritoneal lavage was performed with 1X PBS (DPBS 10X, 14200-067, Gibco, Life Technology) (4 mL) and then cells were recovered by centrifugation at 600xg, 10 min. ELISA for IL1B and IL18 was performed using the supernatant. Exudates were concentrated using Amicon 3K (Merck Millipore) and CD11b⁺ peritoneum exudate cells (PECs) were purified using CD11b magnetic beads according to the manufacturer protocol (130-041-801, Miltenyi biotec). RNA from CD11b⁺ cells were extracted and analysed as described above.

Bone marrow-derived macrophages (BMDMs)

Bone marrow hematopoietic stem cells were isolated from tibia and femur of mice. They were cultured during 1 week in Dulbecco's modified eagle medium (DMEM) without phenol red (ref. 31053-028, Gibco, Life Technology) supplemented with gentamycin (0.4%), L-glutamine (1%) (Sigma-Aldrich, France), 20% L929-conditioned medium (LCM) containing MCSF and 20% fetal bovine serum (FBS). If applicable, cells were pretreated overnight either with hemin (H9039, Sigma-Aldrich) (6 µmol/L) or SR9009 (cat 554726, Merck Millipore) (10 µmol/L) and then co-treated with LPS.

For RNA analysis, macrophages were cultured 3 hours with lipopolysaccharide (LPS) (isotype 0111:B4, Sigma-Aldrich) (100 ng/mL) or 3, 6 or 24 hours with recombinant murine TNFα (315-01A, Peprotech) (50 ng/mL) in DMEM containing 10% FBS. For ELISA, macrophages were first primed with LPS (500 ng/mL) in DMEM containing 10% FBS during 3 hours and then activated for 2 hours with ATP pH7 (A2383, Sigma-Aldrich) (5 mmol/L) in optiMEM + Glutamax (reduced serum medium, 51985-034, Gibco, Life Technology). When applicable, macrophages were treated with MCC950 (CRID3, CP-456773 sodium salt, P20280, Sigma Aldrich) (100 nmol/L), Z-VAD-fmk (20 µmol/L) or z-YVAD-fmk (20 µmol/L) 30 minutes before ATP treatment. For AIM2 inflammasome, cells were treated with poly(dA:dT)/LyoVec™ (tlrl-patc, Invivogen) (2 µg/mL) during 24 hours. The supernatants were collected, cleared by centrifugation, and analysed by ELISA using mouse IL1B (BMS6002TWO, Platinum ELISA affymetrix, eBioscience) and mouse IL18 (BMS618/3, Platinum ELISA affymetrix, eBioscience) kits according to the manufacturer's instructions.

Knockdown of NLRP3 in BMDMs

Experiment were performed as previously described². Briefly, 2x10⁶ differentiated BMDMs were electroporated with *nlrp3* siRNA or control (CTRL) siRNA (Dharmacon, smartpool) using Nucleofector V (Lonza).

Knockdown of NR1D2 in BMDMs

Experiment were performed as previously described². Briefly, 2x10⁶ differentiated BMDMs were electroporated with *rev-erbβ* siRNA or control (CTRL) siRNA (4390817, Ambion by life technologies) using Nucleofector V (Lonza).

Human monocyte-derived macrophages (MDMs)

Human peripheral blood mononuclear cells were isolated from blood of healthy donors by Ficoll density gradient centrifugation. After 7 days of culture in RPMI 1646 (31870-025, Gibco, Life Technology) with gentamycin (40 µg/mL), L-glutamine (2 mmol/L) (Sigma-Aldrich, France), 10% of human serum and macrophage colony-stimulating factor (MCSF, 30 ng/mL) (216-mc/cf, R&D Systems), monocytes were differentiated into macrophages. If applicable, cells were pretreated overnight either with hemin (H9039, Sigma-Aldrich) (6 µmol/L) or SR9009 (cat 554726, Merck Millipore) (10 µmol/L) and then co-treated with LPS.

For RNA analysis, macrophages were cultured with LPS only (100 ng/mL) (L2654, E. coli 026:B6, Sigma-Aldrich) in DMEM during 3 hours.

For ELISA, macrophages were first primed 2 hours with LPS (500 ng/mL) in DMEM and then activated for 1 hour with ATP (A2383, Sigma-Aldrich) (5 mmol/L) in optiMEM + Glutamax (reduced serum medium, 51985-034, Gibco, Life Technology). Macrophages were treated with MCC950 (CRID3, CP-456773 sodium salt, P20280, Sigma Aldrich) (100 nmol/L) 30 minutes before ATP treatment. The supernatants were collected, cleared by centrifugation, and analysed using human IL1B (BMS224/2, Platinum ELISA affymetrix, eBioscience) and human IL18 (BMS267/2, Platinum ELISA affymetrix, eBioscience and ultrasensitive kit 7625 from MBL) kits according to the manufacturer's instructions.

Knockdown of NR1D1 in MDMs

NR1D1 was silenced using a small interferon RNA (siRNA) against *NR1D1* gene *NR1D1* (ref: 1027310, Life Technology) (100 nM) in RPMI containing the transfecting Dharmafect 4 (T-2004-03, Dharmacon) (100 µg/mL).

Knockdown of NR1D2 in MDMs

NR1D2 was silenced using a small interferon RNA (siRNA) against *NR1D2* gene *NR1D2* (43 90 380, Ambion by life technologies) (20 nM) in RPMI containing the transfecting Dharmafect 4 (T-2004-03, Dharmacon) (100 µg/mL).

Synchronized cells

BMDMs or MDMs were synchronized during 2 hours in 50% horse serum. Cells were washed with their respective pre-warmed medium, and incubated for 24 hours in their respective medium (RPMI 10% human serum for MDMs and DMEM 10% SVF for BMDMs) and stopped every 4 hours from 24h to 48h after synchronization. Cells were primed with LPS (L2654, E. coli 026:B6, Sigma-Aldrich) (200 ng/mL) for 3 hours before washing and adding TRIzol.

mRNA analysis

RNAs were isolated from cells using Trizol Reagent (Ambion, Life Technology), were reverse transcribed (4368814, Applied Biosystem) and cDNAs were quantified by quantitative polymerase chain reaction (#600882, Stratagene) on a MX3005 apparatus (Stratagene) using specific primers (see table below). Gene expression was normalized to Cyclophilin gene expression and expressed as described in the figure legends.

Chromatin immunoprecipitation assay (ChIP)

ChIP experiments were performed as previously described² using the anti-NR1D1 (1/50, #13418, Cell Signaling), the anti-H3K27me3 (1/100, ab6002, Abcam) and normal rabbit IgG (1/250, #2729, Cell Signaling) antibodies following manufacturer's instructions.

Protein precipitation

Proteins from conditioned medium were precipitated overnight at 4°C using sodium deoxycholate (0.02%) and trichloroacetate (20%). After centrifugation, protein-containing pellets were washed twice in acetone and resuspended with 60 µL of Laemmli buffer.

Western Blot

50 µg proteins in Laemmli buffer were separated using 10% PAGE and transferred to PVDF membranes. After saturation in 5% bovine serum albumin (BSA), membranes were incubated with the primary antibody directed against NR1D1 (1/1000, Clone 4F6, Abgent), CASP1 (1/1000, Casper1, Adipogen), NLRP3 (1/1000, Cryo-2, Adipogen), IL1B (1/1000, GTX74034, Genetex), Hsp90 (1/1000, sc-1616, Santa Cruz) or actin (1/1000, sc-1616, Santa Cruz) in TBS-BSA solution (2.5%). Then, appropriate HRP-coupled secondary antibody diluted (d1/10000) in 10% skimmed milk (1.15363.0500, Merck Millipore) were used.

Confocal microscopy

BMDMs were permeabilised with 0.1% Triton-X100 and blocked using UV Block buffer (Micom Microtech, cat#TA-125-UB). Primary antibodies against IL18 (1/200, cat#5180R-100, BioVision), CASP1 (1/200, 14-9382, ebioscience), or NLRP3 (1/200, ab4207, Abcam) were incubated overnight. Next, the fluorophore-conjugated secondary antibody (1/500, Alexa antibodies, Thermofischer Scientific) was added. Nuclei were stained with NucBlue fixed cell stain ready probes reagent (DAPI) (Thermofischer Scientific, cat#R37606) according to the manufacturer's instructions. Samples were examined with a LSM880 confocal laser-scanning microscope (Carl Zeiss) and fluorescence intensity was quantified using Fiji software.

ASC speck analysis

Macrophages were plated in 24-well plates and stimulated with LPS (200 ng/mL) for 4 hours. For the last 30 min, BMDM were activated with either ATP (5 mM) or nigericin (20 µmol/L). BMDM were then fixed with 4% paraformaldehyde (PFA) (Thermofisher, cat#28908), permeabilised with PBS-Triton-X100 0.1% and blocked using UV Block buffer. Primary antibodies against ASC (1/500, ADI-905-173, Adipogen) were incubated overnight, before the fluorophore-conjugated secondary antibody (1/500, Alexa antibodies, Thermofischer Scientific) was added. Nuclei were stained with NucBlue fixed cell

stain ready probes reagent (DAPI) (ThermoFischer Scientific, cat#R37606) according to the manufacturer's instructions. Samples were examined with a Nikon Ti epifluorescence microscope (Carl Zeiss) using 40x magnification. ASC specks were then quantified in at least 200 cells.

Peritonitis

Nr1d1^{-/-} and *Nr1d1^{+/+}* male mice were intraperitoneally injected first with the NLRP3 inhibitor MCC950 (CRID3, CP-456773 sodium salt, PZ0280, Sigma Aldrich) (50 mg/kg) or saline. After 30 minutes, mice received an intraperitoneal injection of LPS (isotype 0111:B4, Sigma-Aldrich) (100 µg or 3.5 mg/Kg). 2 hours later, mice were then injected with alum (prod#77161, Thermo Scientific) (700 µg). Blood was collected from retro-orbital route and plasma was separated from cellular fraction by centrifugation. Peritoneal lavages were performed after 4 hours with sterile ice-cold PBS1x (DPBS 10X, 14200-067, Gibco, Life Technology) (4mL). Samples were concentrated with Amicon 3K (Merck Millipore); plasma and exudate IL1B and IL18 protein amounts were then quantified by ELISA.

Fulminant hepatitis

To analyse the circadian behaviour of survival rate and time upon LPS/D-Galactosamine injection, 8 week-old C57/Bl6 female mice were challenged with intraperitoneal injection of LPS (isotype 0111:B4, Sigma-Aldrich) (15 µg/kg) and D-Galactosamine hydrochloride (Sigma-Aldrich) (575 mg/kg) every 4 hours (ZT0, ZT4, ZT8, ZT12, ZT16, ZT20 and ZT4) and monitored for their survival duration and rate every 30 minutes for 48 hours.

To investigate the effect of NR1D1 on fulminant hepatitis parameters, *Nr1d1^{-/-}* and *Nr1d1^{+/+}* male mice were intraperitoneally injected at ZT1.5 first with the NLRP3 inhibitor MCC950 (CRID3, CP-456773 sodium salt, PZ0280, Sigma Aldrich) (50 mg/kg) or saline. After 30 minutes at ZT2, mice received an intraperitoneal injection of LPS (isotype 0111:B4, Sigma-Aldrich) (15 µg/kg) and D-Galactosamine hydrochloride (Sigma-Aldrich) (575 mg/kg). For Rev-erb pharmacological activation experiment with SR9009, 8-week old C57/Bl6 female mice were pretreated with an intraperitoneal injection of the SR9009 Rev-erb agonist (100 mg/kg) (Merck-Millipore) or 15% cremaphor (Sigma-Aldrich) as vehicle at ZT11 on the day (day0) preceding the induction of the acute hepatic injury. Then, at day1, mice were intraperitoneally co-injected at ZT1.5 with either SR9009 (100 mg/kg) or 15% cremaphor and with the NLRP3 inhibitor MCC950 (CRID3, CP-456773 sodium salt, PZ0280, Sigma Aldrich) (50

mg/kg) or saline. After 30 minutes at ZT2, mice received an intraperitoneal injection of PBS as control, or LPS (isotype 0111:B4, Sigma-Aldrich) (15 µg/kg) and D-Galactosamine hydrochloride (Sigma-Aldrich) (575 mg/kg). To determine the survival rate, mice were monitored every 30 minutes after LPS/D-GalN injection for 48 hours. In other experiments, mice were sacrificed 5 hours after LPS/D-GalN administration, blood was collected from retro-orbital route and plasma were separated from cellular fraction by centrifugation to determine plasma ALAT activity (Thermo-fisher). Livers were pictured and harvested for further analysis. The median lobe was embedded in cryogenic OCT medium (NEG50, 6502G, Richard-Allan Scientific) and stored at -80°C for further analysis. 10-µm sections were stained with FAM-FLICA according to the manufacturer indications (Immunochemistry Technologies) and caspase-1 activity was quantified in three different tissue sections of each mouse with a LSM 880 confocal laser-scanning microscope at a 40x magnification (Carl Zeiss). mRNAs from the right posterior lobe were extracted using the Chomczynski and Sacchi methods³. The left lobe was fixed in formaldehyde 4% and embedded in paraffin. 3-µm sections were stained with eosin and hematoxylin and were visualised using Nikon Eclipse Ti at 20x magnification to evaluate hemorrhage.

Pharmacological treatment experiments

Bone marrow hematopoietic cells were isolated from mice as indicated above. For RNA analysis, BMDMs were either pre-treated with the SR9009 Rev-erb agonist (10 µmol/L) for 12 hours and treated with LPS (100 ng/mL) for 3 hours or were cultured with LPS (100 ng/mL) in DMEM containing 10% FBS for 3 hours and treated with SR9009 (10 µM) or vehicle (DMSO) for 12 hours. For protein analysis and western blotting, BMDM were primed with IFN γ (100 ng/mL) and LPS (10 ng/mL) for 12 hours and treated with SR9009 (10 µmol/L) or vehicle (DMSO) for 12 hours. For ELISA, BMDMs were primed with LPS (100 ng/mL) for 3 hours in DMEM containing 10% FBS, followed by treatment with Rev-erb agonist SR9009 (10 µmol/L) or vehicle (DMSO) for 12 hours. Macrophages were then treated with MCC950 (100 nM) in optiMEM (reduced serum medium, 31985088, Life Technologies) for 1 hour and activated with ATP (5 mmol/L) for 2 hours. The supernatants were collected and cleared by centrifugation. ELISA for mouse IL1B (BMS6002TWO, Platinum ELISA affymetrix, eBioscience) and mouse IL18 (BMS618/3, Platinum ELISA affymetrix, eBioscience) were performed according to the manufacturer's instructions.

For peritonitis experiments, 12 week-old male C57Bl/6 mice (n=10 per group) were intraperitoneally injected with the SR10067 Rev-erb agonist (25 mg/kg) or vehicle at 5 am (ZT23). Mice were then intraperitoneally injected with LPS one hour after SR10067 injection at ZT0 and every six hours after that at ZT6, ZT12, ZT18. Mice were sacrificed 4 hours after LPS injection (ZT4, ZT10, ZT16, ZT22) and peritoneal lavage was performed with sterile PBS 1x (10mL). Exudate cells were cultured in DMEM containing 10% FBS and supernatant were collected after 2 hours (time indicated on the figure axis). Supernatant were cleared by centrifugation and ELISA was performed according to the manufacturer's instructions (SMLB00C, R&D Systems;7625, R&D Systems). SR9009 and SR10067 were synthesized as previously described^{4,5}.

Fluorescence-Activated Cell Sorting (FACS) analysis

8-week old C57/Bl6 female mice were pretreated with an intraperitoneal injection of the SR9009 Rev-erb agonist as described above. The next morning, mice were intraperitoneally co-injected at ZT2 with either SR9009 (100 mg/kg) or 15% cremaphor and with the NLRP3 inhibitor MCC950 (CRID3, CP-456773 sodium salt, PZ0280, Sigma Aldrich) (50 mg/kg) or saline. After 30 minutes, mice received an intraperitoneal injection of PBS as control, or LPS (isotype 0111:B4, Sigma-Aldrich) (15 µg/kg) and D-Galactosamine hydrochloride (Sigma-Aldrich) (575 mg/kg). 5 hours later, livers were collected, weighted, minced and digested in RPMI containing collagenase type D (11 088 882, 0.233U/mg, Roche) (1 mg/mL) during 20 minutes at 37°C while thoroughly agitated. After adding EDTA (2 mM), livers were mechanically homogenised using a 21G needle and a 70 µm cell strainer. Cellular fraction was then washed using PBS + BSA 0.5%. Liver homogenates were resuspended in an 40% Percoll™ (17-0891-01, density 1.129 g/mL, GE Healthcare) and loaded on a 80% Percoll™ phase. After centrifugation, the cell ring was harvested and washed. The red blood cells were eliminated by an incubation in RBC lysis buffer. Cells were filtered through a 40 µm cell trainer and counted. Cells were labelled by the following antibodies (BD and Biolegend), used to identify and quantify immune cells by FACS (BD LSRFortessa™ X20, BD Bioscience): CD45.2, CCR2, CD115, Ly6C and F4/80. Alived cells were stained using Zombie UV™ Fixable Viability Kit (423107, BioLegend).

***In silico* analysis**

Retrieval of putative RevRE in sequences of *I11β* and *Nlrp3* promoters has been performed using MatInspector (Genomatix). Sequencing data (ChIPseq and 5'GROseq) were obtained from Gene Expression Omnibus (GSE45914) and analyzed with Integrated Genome Browser (IGB)⁶.

Statistical analysis

Statistical analysis was performed on GraphPad Prism software using Student's *t*-test for comparisons between two groups, and one-way or two-way ANOVA with Bonferroni post-hoc multiple comparisons for assessment of more than two groups and cosinor analysis for circadian experiment. Survival rate and time were compared by Kaplan-Meier analysis, a log-rank Mantel-Cox and a log-rank test were performed to analyse the survival time and rate, respectively, as indicated in figure legends.

REFERENCE

1. Zhang Y, Fang B, Emmett MJ, et al. GENE REGULATION. Discrete functions of nuclear receptor Rev-erbalpha couple metabolism to the clock. *Science* 2015;348:1488-92.
2. Pourcet B, Feig JE, Vengrenyuk Y, et al. LXRalpha regulates macrophage arginase 1 through PU.1 and interferon regulatory factor 8. *Circ.Res.* 2011;109:492-501.
3. Chomczynski P, Sacchi N. The single-step method of RNA isolation by acid guanidinium thiocyanate-phenol-chloroform extraction: twenty-something years on. *Nat Protoc* 2006;1:581-5.
4. Banerjee S, Wang Y, Solt LA, et al. Pharmacological targeting of the mammalian clock regulates sleep architecture and emotional behaviour. *Nat.Commun.* 2014;5:5759.
5. Solt LA, Wang Y, Banerjee S, et al. Regulation of circadian behaviour and metabolism by synthetic REV-ERB agonists. *Nature* 2012;485:62-68.
6. Lam MT, Cho H, Lesch HP, et al. Rev-Erbs repress macrophage gene expression by inhibiting enhancer-directed transcription. *Nature* 2013;498:511-515.

SUPPLEMENTARY TABLE 1

qPCR primers and ChIP primers used in this study

h, human; m, mouse

Gene name	Sense / antisense	Sequence
<i>mI18</i>	Forward	TCTGACATGGCAGCCATTGT
	Reverse	CAGGCCTGACATCTTCTGCAA
<i>mI1β</i>	Forward	GCCACCTTTTGACAGTGATGAG
	Reverse	CCTGAAGCTCTTGTGATGTGC
<i>mCaspase-1</i>	Forward	ACCCTCAAGTTTTGCCCTTT
	Reverse	GATCCTCCAGCAGCAACTTC
<i>mNLRP3</i>	Forward	CCCTTGGAGACACAGGACTC
	Reverse	GAGGCTGCAGTTGTCTAATTCC
<i>mNr1d1</i>	Forward	TGGCCTCAGGCTTCCACTATG
	Reverse	CCGTTGCTTCTCTCTTGGG
<i>mNr1d2</i>	Forward	AGTAGGTGGATGTTCTCAGACTGAGA
	Reverse	ATGGAGACTTGCTCATAGGACACAC
<i>mARNTL</i>	Forward	CCAACCGTGGCTCCAACCTT
	Reverse	CTAGGTGCTTGTGCTTGTGT
<i>mAIM2</i>	Forward	AGGCAGTGGGAACAAGACAG
	Reverse	GAAAACCTCCTGACGCCACC
<i>mTNFα</i>	Forward	GTCTACTGAACTTCGGGGTGA
	Reverse	CTCCTCCACTTGGTGGTTTG
<i>mCcl2</i>	Forward	GCCAACTCTCACTGAAGCC
	Reverse	GCTGGTGAATGAGTAGCAGC
<i>mF4/80</i>	Forward	CTTTGGCTATGGGCTTCCAGTC
	Reverse	GCAAGGAGGACAGAGTTTATCGTG
<i>hNLRP3</i>	Forward	CATGAGTGCTGCTTCGACAT
	Reverse	CGACTCCTGAGTCTCCAAG
<i>hIL1B</i>	Forward	GACCTGAGCACCTTCTTCCCTTC
	Reverse	GCAGTTCAGTGATCGTACAGGTGC
<i>hIL18</i>	Forward	GCTGAAGATGATGAAAACCTGGA
	Reverse	GAGGCCGATTTCTTGGTCA
<i>hNR1D1</i>	Forward	CTGCAAGGGCTTTTTCCGT
	Reverse	ATGCGGACGATGGAGCAAT
<i>hNR1D2</i>	Forward	ACAAGCAAATCGAGTGACCTG
	Reverse	CTCCATAGTGGAACTCCTGACGC
<i>hARNTL</i>	Forward	TGCCACCAATCCATACACAGAA
	Reverse	TCCATCTGCTGCCCTGAGA
<i>Cyclophilin</i>	Forward	GCATACGGGTCTGGCATCTTGCC

	Reverse	ATGGTGATCTTCTTGCTGGTCTTGC
ChIP arntl	Forward	GGAAAGTAGGTTAGTGGTGCGAC
	Reverse	CAAGTCCGGCGCGGGTAAACAGG
ChIP NLRP3 - 4.4kb	Forward	TAGGAAGCATGGGGATTGTC
	Reverse	GAACAAAGTGGTGTATACTGTTCTGA
ChIP NLRP3 - 4.2kb	Forward	GAGCACTGCCTGTTCTCCA
	Reverse	TGTTCTGAGGAGGAATTGTGC
ChIP NLRP3 - 1.2kb	Forward	GTTCACGTCTTGAAGCCACA
	Reverse	CCAGATAGCAGCCTTGGGTA
ChIP NLRP3 - 0.2kb	Forward	ATGCACACAATTCCACCTGA
	Reverse	CAGAGCACCAAGGTGAGGAC
ChIP NLRP3 TSS	Forward	CACGAGTCCTGGTGACTTTG
	Reverse	GAGCCATGGAAGAAAAGTTCC
ChIP <i>Il1β</i> -4.0kb	Forward	ATGTCCCTGCCCTGATTGT
	Reverse	CCAAAGAAATTTGGGGAAGA
ChIP <i>Il1β</i> -2.4kb	Forward	GGGGTGTGGCATAGTGATGA
	Reverse	AGTGCCCGTCACCATCCT
ChIP <i>Il1β</i> -0.15kb	Forward	GGAAGAGGCTATTGCTACCC
	Reverse	CCATTTCCACCACGATGAC

SUPPLEMENTARY FIGURE LEGEND

Supplementary Figure 1: Cosinor analysis of mRNA and cytokine oscillation (A) CD11b⁺ PEC mRNA (B) CD11b⁺ PEC ELISA (C) synchronised BMDM and (D) synchronised human MDM.

Supplementary Figure 2: Gene expression of the NLRP3 inflammasome pathway displays circadian oscillations in synchronized mouse BMDMs and human MDMs. (A) *Nr1d1*, (B) *Nr1d2*, (C) *Arntl*, (D) *Nlrp3* and (E) *Il18* mRNA levels in BMDMs from *Nr1d1*^{+/+} or *Nr1d1*^{-/-} mice that were synchronized *in vitro* by serum shock. Data are means ± SD (n=3). *p<0.05, **p<0.01, ***p<0.001 as determined by two-way ANOVA and Bonferroni post-hoc test to compare *Nr1d1*^{+/+} or *Nr1d1*^{-/-} mice. ¶p<0.01, ¶¶p<0.001 as determined by one-way ANOVA to assess variation over time in *Nr1d1*^{+/+} cells, and \$\$\$p<0.001 as determined by one-way ANOVA to assess variation over time in *Nr1d1*^{-/-} cells, (F) *NR1D1*, (G) *NR1D2*, (H) *ARNTL*, (I) *NLRP3* and (J) *IL18* mRNA levels in human MDMs that were synchronized by serum shock. Data are means ± SD (n=3). †p<0.05, ‡p<0.01, ¶¶p<0.001 as determined by one-way ANOVA to assess variation over time in human MDMs

Supplementary Figure 3: NR1D1 regulates *Nlrp3* expression. (A) Analysis of ChIPseq and 5'Gro-seq data from²³ showing that NR1D1 binds to and represses transcription from the *Nlrp3* promoter in rev-erba overexpressing RAW264.7 macrophages. (B) *Nr1d1*, (C) *Nr1d2*, (D) *Nlrp3*, (E) *Il1β* and (F) *Il18* mRNA levels in BMDMs treated with LPS during 1 hour (LPS 1h) or not (Ctrl) (n=3). **p<0.001 as determined by unpaired *t*-test. (G) Quantification of NLRP3 protein expression from NLRP3 immunofluorescence in LPS-primed BMDMs from *Nr1d1*^{+/+} or *Nr1d1*^{-/-} mice (n=3). Data are mean values ± SD (at least 150 cells per slide). ***p<0.001 as determined by unpaired two-tailed *t*-test.

Supplementary Figure 4: Both NR1D1 and NR1D2 regulate the NLRP3 inflammasome pathway in human MDMs. (A) *Nr1d1* and (B) *Nr1d2* mRNA levels in LPS-primed (LPS) or not (CTRL) BMDMs from *Nr1d1*^{+/+} or *Nr1d1*^{-/-} mice transfected with siRNA against *Nr1d2* (siNr1d2) or a scrambled siRNA (siCtrl). (C) *NLRP3*, (D) *IL1β*, (E) *NR1D1*, (F) *NR1D2* mRNA levels in LPS-primed (LPS) or not (CTRL) human MDMs and (G) IL1B and (H) IL18 secretion in LPS-primed and ATP-activated (ATP) or not (CTRL) human MDMs transfected with a siRNA against *Nr1d1* (siRα) and/or *Nr1d2* (siRβ) or a

scrambled siRNA (siCtrl). Data are mean values \pm SD (n=3). Vs siCtrl **p<0.01, ***p<0.001 as determined by two-way ANOVA followed by a Bonferroni post-hoc test. Vs siRNA *Nr1d1* siRNA *Nr1d2* *p<0.01, **p<0.001 as determined by two-way ANOVA followed by a Bonferroni post-hoc test.

Supplementary Figure 5: NR1D1 does not regulate the AIM2 inflammasome. (A) *Aim2* mRNA levels in LPS-primed (LPS) or not (CTRL) BMDMs from *Nr1d1^{+/+}* or *Nr1d1^{-/-}* mice. (B) IL1B and (C) IL18 secretion in LPS-primed (LPS) or not (/) and activated with ATP (ATP) or Poly(dA:dT) BMDMs from *Nr1d1^{+/+}* or *Nr1d1^{-/-}* mice. Data are mean values \pm SD (n=3). ***p<0.001 as determined by two-way ANOVA and Bonferroni post-hoc test.

Supplementary Figure 6: NR1D1 deficiency leads to increased Caspase-1 maturation, but not expression, in primary macrophages. (A-B) Caspase-1 (CASP1) mRNA (A) and protein (B) levels in control (CTRL) or LPS-primed (LPS) BMDMs from *Nr1d1^{+/+}* or *Nr1d1^{-/-}* mice (n=3). Immunofluorescence quantification on at least 150 cells per slide. (C) Total proteins were visualized in the acrylamide gel after a coomassie blue staining as a loading control for Figure 3A in BMDM isolated from *Nr1d1^{+/+}* (*R α ^{+/+}*) and *Nr1d1^{-/-}* (*R α ^{-/-}*) mice. (D) Western blot quantification of secreted mature Caspase-1 p20 and p10 protein fragments from *Nr1d1^{+/+}* or *Nr1d1^{-/-}* mice BMDMs treated with LPS (CTRL) or with LPS and ATP (ATP). Data are means \pm SD (n=3). *p<0.05, as determined by two-way ANOVA and Bonferroni post-hoc test.

Supplementary Figure 7: NR1D1 deficiency increases IL1B and IL18 secretion in primary macrophages. (A) IL1B secretion in LPS-primed (LPS) and ATP-activated (LPS ATP) human MDMs in which *Nr1d1* has been silenced (siNr1d1). (B) IL1B and (C) IL18 secretion in LPS-primed (LPS) and ATP-activated (LPS ATP) BMDMs from *Nr1d1^{+/+}* or *Nr1d1^{-/-}* mice. Data are means \pm SD (n=3). **p<0.01, ***p<0.001 as determined by two-way ANOVA and Bonferroni post-hoc test.

Supplementary Figure 8: NR1D1 pharmacological activation downregulates the NLRP3 inflammasome pathway. (A) IL1B secretion in LPS-primed (LPS) and ATP-activated (LPS ATP) human MDMs treated with Hemin or not (Vehicle). (B) NLRP3 protein quantification of Fig. 5.B in LPS-primed (LPS) or not (CTRL) BMDMs treated with SR9009 or DMSO as control. (C) *NLRP3* (D) *IL1 β*

and (E) *IL18* mRNA levels in LPS-primed (LPS) or not (CTRL) human MDMs treated with Hemin or not (Vehicle). Data are means \pm SD (n=3). ***p<0.001 as determined by two-way ANOVA and Bonferroni post-hoc test.

Supplementary Figure 9: NR1D1 controls IL1B and IL18 secretion in a Caspase 1-dependent manner. (A) IL18 secretion in LPS-primed (CTRL) and ATP-activated (ATP) BMDMs from *Nr1d1^{+/+}* or *Nr1d1^{-/-}* mice. (B) IL1B secretion in LPS-primed (CTRL) and ATP-activated (ATP) in human MDMs in which *Nr1d1* has been silenced (si*Nr1d1*). These samples were treated with a caspase 1 inhibitor Z-YVAD-fmk or not (Vehicle). Data are means \pm SD (n=3). **p<0.01, ***p<0.001 as determined by two-way ANOVA and Bonferroni post-hoc test. (C) Intracellular IL18 protein in LPS-primed BMDMs from *Nr1d1^{+/+}* or *Nr1d1^{-/-}* mice (n=3). Quantification of intracellular IL18 from 150 cells/slide. Data are means \pm SD. ***p<0.001 as determined by unpaired two-tailed student *t*-test.

Supplementary Figure 10: NR1D1 binds to the *il1 β* promoter and inhibits de novo transcription. Analysis of ChIPseq and 5'Gro-seq data from Lam et al.²³ showing that NR1D1 binds to and represses transcription from the *Il1 β* promoter in *rev-erba*-overexpressing RAW264.7 macrophages.

Supplementary Figure 11: NR1D1 prevents the development of fulminant hepatitis in a NLRP3-dependent manner. (A) Liver *Ccl2* and (C) *Tnfa* mRNA levels, and (B) secreted IL1B in blood sampled from *Nr1d1^{+/+}* and *Nr1d1^{-/-}* mice pre-treated with MCC950 or saline and then injected with LPS/GalN. Data are means \pm SEM (n=5-6). *p<0.05, **p<0.01 as determined by two-way ANOVA and Bonferroni post-hoc test. (D-E) *Nlrp3* (D) and *Il1 β* mRNA (E) levels in BMDMs from *Nr1d1^{+/+}* and *Nr1d1^{-/-}* mice primed with TNF α during 3, 6 or 24 hours. Data are means \pm SD (n=3). (F) Hemorrhage area in liver, (G) Representative liver appearance, (H) Secreted IL1B in blood samples, and (I) Liver *Ccl2* and (J) *Tnfa* and mRNA levels from mice pre-treated with SR9009 or Vehicle and MCC950 or Saline, and then intraperitoneally challenged with LPS plus D-Galactosamine (GalN). Data are means \pm SEM (n=5-6). Data are means \pm SEM. *p<0.05, **p<0.01, ***p<0.001 as determined by two-way ANOVA and Bonferroni post-hoc test.

Supplementary Figure 12: NR1D1 pharmacological activation reduces leukocytes recruitment to the liver in fulminant hepatitis. C57/Bl6 mice were pre-treated with SR9009/DMSO and/or MCC950/Vehicle and then challenged with LPS/GalN or PBS as control (Ctrl). Immune cells were isolated on a percoll gradient, counted and analyzed by FACS analysis. **(A)** Leukocytes, **(B)** monocytes (CCR2⁺CD115⁺), **(C)** infiltrating monocytes (CCR2⁺Ly6C^{high}), **(D)** macrophages (F4/80⁺) and **(E)** recruited macrophages (F4/80⁺CCR2⁺Ly6C^{high}) number per g of liver. **(F)** Quantification and **(G)** Representative neutrophil staining (Ly6G⁺) on liver sections. Data are means ± SEM (n=6). **p<0.01, ***p<0.001 as determined by two-way ANOVA and Bonferroni post-hoc test. **(H)** *Nlrp3* **(I)** *Il1β* and **(J)** *Il18* mRNA levels in F4/80⁺ cells. Data are means ± SEM (n=6). *p<0.05, **p<0.01 as determined by two-way ANOVA and Bonferroni post-hoc test.

Supplementary Figure 13: Scheme depicting how NR1D1 regulates the NLRP3 inflammasome pathway.

FIGURE 1

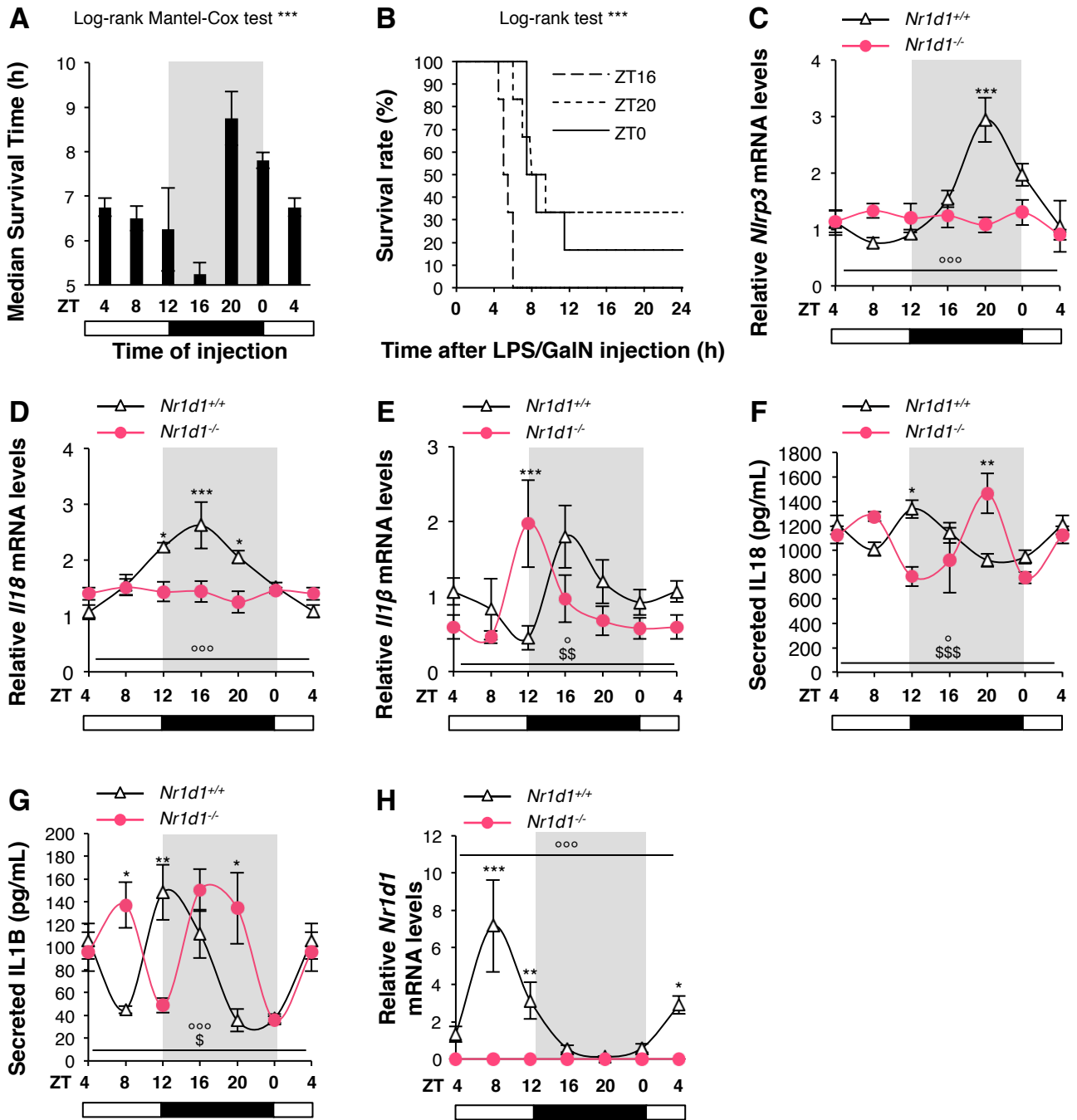


Figure 1: NR1D1 controls daily variations in *Nlrp3* expression and activation, and IL1B and IL18 secretion.

(A) Survival time and (B) Survival rate after FH induction every for 4 hours. Data are means \pm SEM (n=4). ***p<0.001 as determined by Log-rank Mantel Cox (A) and Log-rank (B) test. (C) *Nlrp3*, (D) *Il18*, (E) *Il1β* and (H) *Nr1d1* mRNA levels in CD11b⁺ PECs from unstimulated *Nr1d1*^{+/+} or *Nr1d1*^{-/-} mice obtained by peritoneal lavage around the clock (ZT4→ZT4). (F) Secreted IL18 and (G) IL1B in peritoneal lavages from unstimulated *Nr1d1*^{+/+} or *Nr1d1*^{-/-} mice around the clock (ZT4→ZT4). Data are means \pm SEM (n=4-7). *p<0.05, **p<0.01, ***p<0.001 as determined by two-way ANOVA and Bonferroni post-hoc test to compare *Nr1d1*^{+/+} and *Nr1d1*^{-/-}. °p<0.05, °°p<0.01, °°°p<0.001 as determined by one-way ANOVA test to compare *Nr1d1*^{+/+}. \$p<0.05, \$\$p<0.01, \$\$\$p<0.001 as determined by one-way ANOVA test to compare *Nr1d1*^{-/-}. Cosinor analysis is given in Supplementary Figure 1. ZT0: lights on, ZT12: lights off.

FIGURE 2

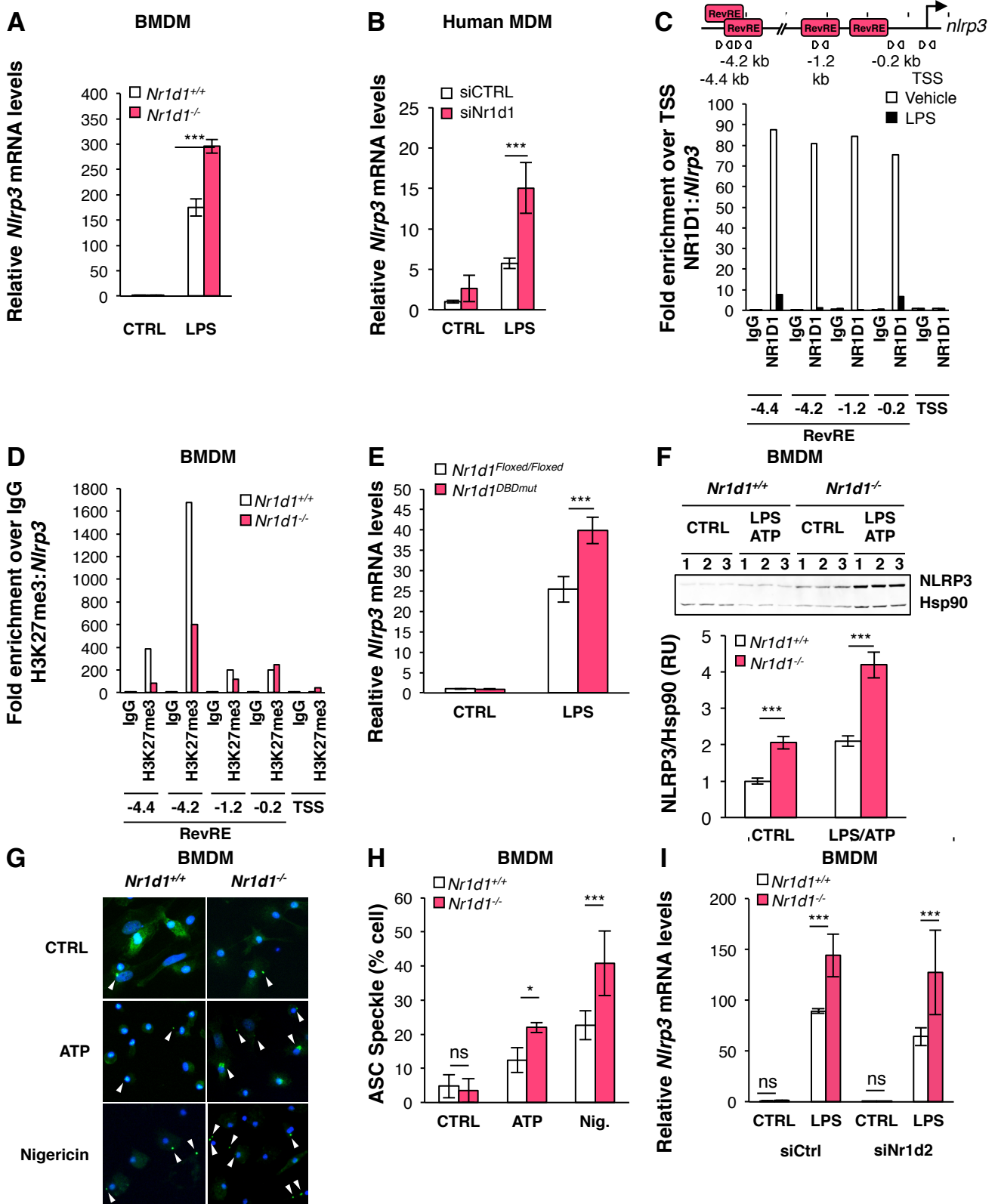


Figure 2: NR1D1 directly regulates the NLRP3 inflammasome in macrophages.

Nlrp3 mRNA levels in control (CTRL) and LPS-primed (LPS) (A) BMDMs from $Nr1d1^{+/+}$ and $Nr1d1^{-/-}$ mice and in (B) MDMs transfected with siRNA against *Nr1d1* (siNr1d1) or a scrambled siRNA (siCTRL) (n=3). Data are represented as means \pm SD. ***p < 0.001 as determined by two-way ANOVA followed by a Bonferroni post-hoc test. (C) ChIP analysis of NR1D1 occupancy to the *Nlrp3* promoter in control (Vehicle) or LPS-primed (for 1 hour) BMDMs. The top diagram represents putative Rev-erb Response Elements (RevREs) unveiled by MatInspector promoter analysis. Down, ChIP analysis from one representative experiment. (D) ChIP analysis of H3K27me3 at the *Nlrp3* promoter in $Nr1d1^{+/+}$ and $Nr1d1^{-/-}$ BMDMs. (E) *Nlrp3* mRNA levels in BMDMs from $Nr1d1^{Flxed/Flxed};LysM^{Cre/+}$ ($Nr1d1^{Flxed/Flxed}$) or $Nr1d1^{Flxed/Flxed};LysM^{Cre/+};Nr1d1^{DBDmut}$ ($Nr1d1^{DBDmut}$) mice. (F) NLRP3 protein expression in control (CTRL) and LPS-primed ATP-activated (LPS ATP) BMDMs from $Nr1d1^{+/+}$ or $Nr1d1^{-/-}$ mice (n=3). Top, the western blot and down, its quantification. ***p < 0.001 as determined by two-way ANOVA followed by a Bonferroni post-hoc test. (G) ASC specks formation and (H) its quantification in LPS-primed BMDMs from $Nr1d1^{+/+}$ and $Nr1d1^{-/-}$ mice treated with ATP, Nigericin or vehicle (CTRL). Results are presented as mean percentage of cells displaying ASC specks \pm SD. *p < 0.05, ***p < 0.001 as determined by two-way ANOVA followed by a Bonferroni post-hoc test. (I) *Nlrp3* mRNA levels in BMDMs from $Nr1d1^{+/+}$ and $Nr1d1^{-/-}$ mice transfected with siRNA against *Nr1d2* (siNr1d2) or a scrambled siRNA (siCtrl) (n=3). Data are represented as means \pm SD. ***p < 0.001 as determined by two-way ANOVA followed by a Bonferroni post-hoc test.

FIGURE 3

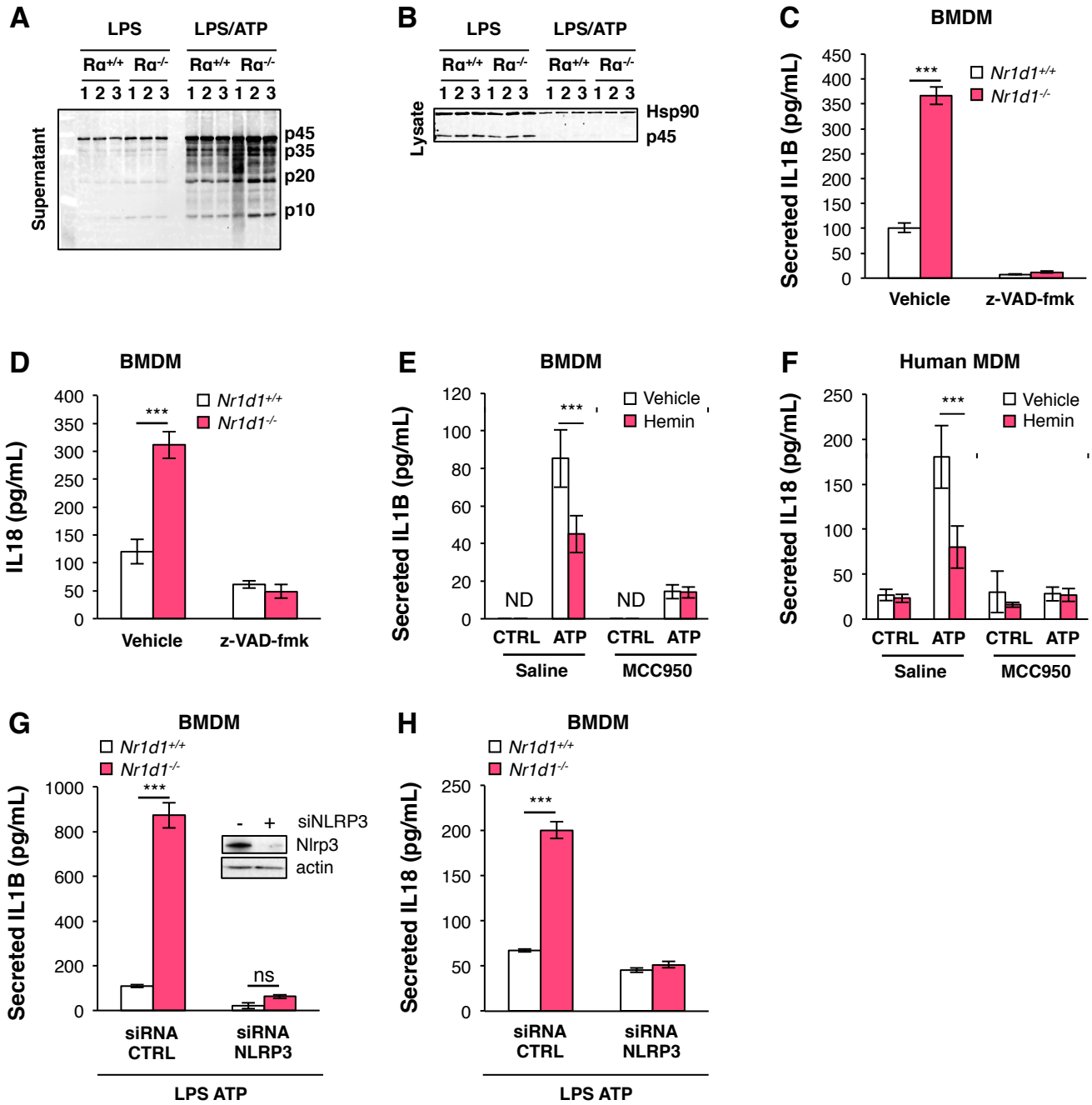


Figure 3: NR1D1 regulates IL18 and IL1B maturation and secretion in a NLRP3 inflammasome-dependent manner.

Caspase-1 protein (sub-unit p10, p20, p35, p45) expression in supernatant (A) or lysate (B) from LPS-primed (LPS) and ATP-activated (LPS/ATP) or not (*I*) BMDMs from *Nr1d1*^{+/+} (*Ra*^{+/+}) and *Nr1d1*^{-/-} (*Ra*^{-/-}) mice (representative of 3 independent experiments). (C) IL1B and (D) IL18 secreted by LPS-primed and ATP-activated BMDMs isolated from *Nr1d1*^{+/+} and *Nr1d1*^{-/-} mice that were treated with low dose of caspase inhibitor z-VAD-fmk (z-VAD-fmk) or not (Vehicle) (n=3). (E) IL1B secreted by LPS-primed and ATP activated (ATP) or not (CTRL) BMDMs treated with (hemin) or its vehicle (vehicle) and with NLRP3 inhibitor MCC950 or not (Saline) (n=3). (F) IL18 secreted by LPS-primed and ATP-activated (ATP) or not (CTRL) MDMs treated with (hemin) or its vehicle (vehicle) and with NLRP3 inhibitor MCC950 or not (Saline) (n=3). (G) IL1B and (H) IL18 secreted by LPS-primed and ATP-activated BMDMs isolated from *Nr1d1*^{+/+} and *Nr1d1*^{-/-} mice in which NLRP3 was silenced (siRNA NLRP3) or not (siRNA CTRL) (n=3). The top western blot (G) shows NLRP3 protein silencing. Data are represented as means ± SD. ***p<0.001 as determined by two-way ANOVA followed by a Bonferroni post-hoc test.

FIGURE 4

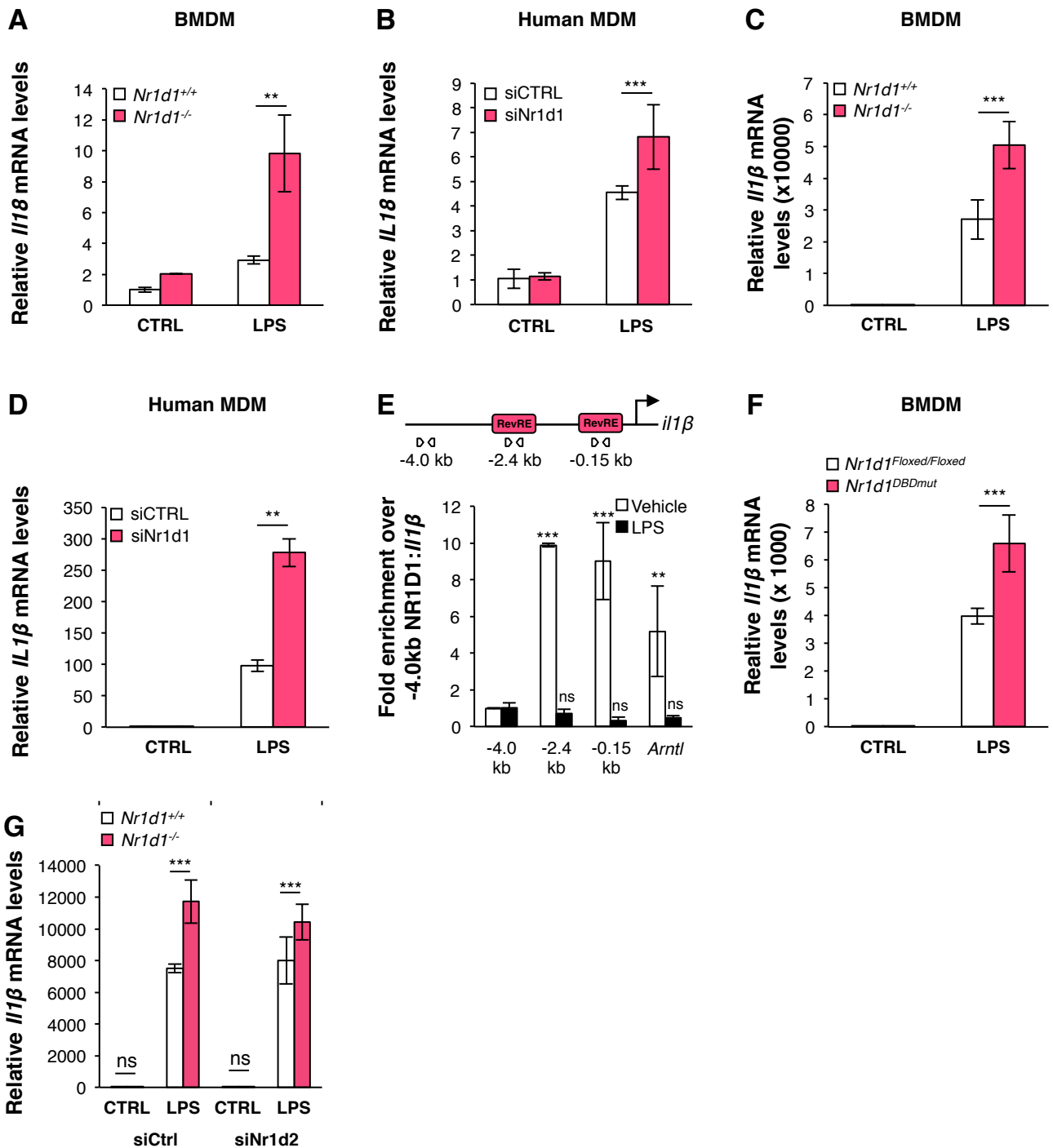


Figure 4: NR1D1 regulates IL18 and IL1B expression.

(A-D) *Il18* (A,B) and *Il1β* (C,D) mRNA levels in LPS-primed BMDMs isolated from $Nr1d1^{+/+}$ or $Nr1d1^{-/-}$ mice (A,C) and in LPS-primed human MDMs transfected with siRNA against *Nr1d1* (siNr1d1) or a scrambled siRNA (siCTRL) (B,D) (n=3). Data are represented as means \pm SD. **p<0.01, ***p<0.001 as determined by two-way ANOVA followed by a Bonferroni post-hoc test. (E) ChIP analysis of NR1D1 occupancy at the *Il1β* and *Arntl* promoter (as control) in control (Vehicle) or LPS-primed (for 1 hour) BMDMs (n=3). The top diagram represents putative Rev-erb Response Elements (RevREs) unveiled by MatInspector promoter analysis. Data are represented as means \pm SD. **p<0.01, ***p<0.001 as determined by an unpaired t-test. *Il1β* mRNA levels in LPS-primed (F) BMDMs isolated from $Nr1d1^{Floxed/Floxed};LysM^{+/+}$ ($Nr1d1^{Floxed/Floxed}$) or $Nr1d1^{Floxed/Floxed};LysM^{Cre/+}$ ($Nr1d1^{DBDmut}$) mice and (G) BMDMs from $Nr1d1^{+/+}$ and $Nr1d1^{-/-}$ mice transfected with siRNA against *Nr1d2* (siNr1d2) or a scrambled siRNA (siCtrl) (n=3). Data are represented as means \pm SD. ***p<0.001 as determined by two-way ANOVA followed by a Bonferroni post-hoc test.

FIGURE 5

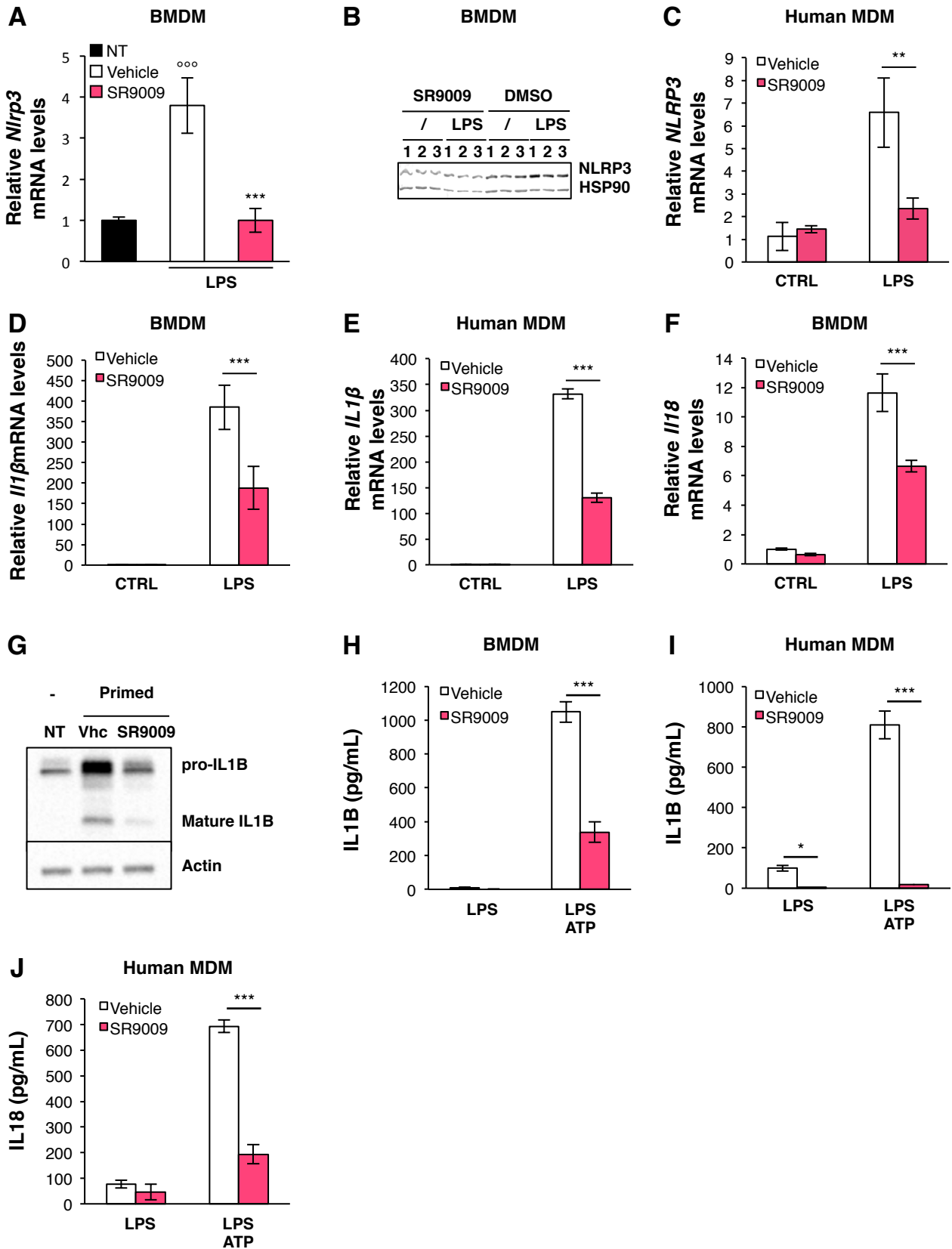


Figure 5: NR1D1 pharmacological activation inhibits the NLRP3 inflammasome pathway in primary macrophages.

(A) *Nlrp3* mRNA levels in LPS-primed (LPS) or not (NT) BMDMs treated with SR9009 (n=3). (B) NLRP3 protein levels in LPS-primed (LPS) or not (I) BMDMs treated with SR9009 or DMSO (representative of 3 independent experiments). (C) *NLRP3* and (E) *Il1β* mRNA levels in LPS-primed human MDMs pre-treated with SR9009 or not (Vehicle) (n=3). (D) *Il1β* and (F) *Il18* mRNA levels in LPS-primed BMDMs pre-treated or not with SR9009 (n=3). (G) pro- and matured IL1B protein expression in LPS-primed BMDM or not (NT) and treated with SR9009 or not (Vhc). (H) IL1B secretion in LPS-primed and ATP-activated BMDMs pre-treated with SR9009 or not (Vehicle) (n=3) (I) IL1B and (J) IL18 secretion in LPS-primed and ATP-activated human MDMs pre-treated with SR9009 or not (Vehicle) (n=3). Data are represented as means ± SD. ***p<0.001 in LPS vs unstimulated vehicle condition (A); *p<0.05, **p<0.01, ***p<0.001 as determined by one-way ANOVA (A) or two-way ANOVA (C-F, H-J) followed by a Bonferroni post-hoc test.

FIGURE 6

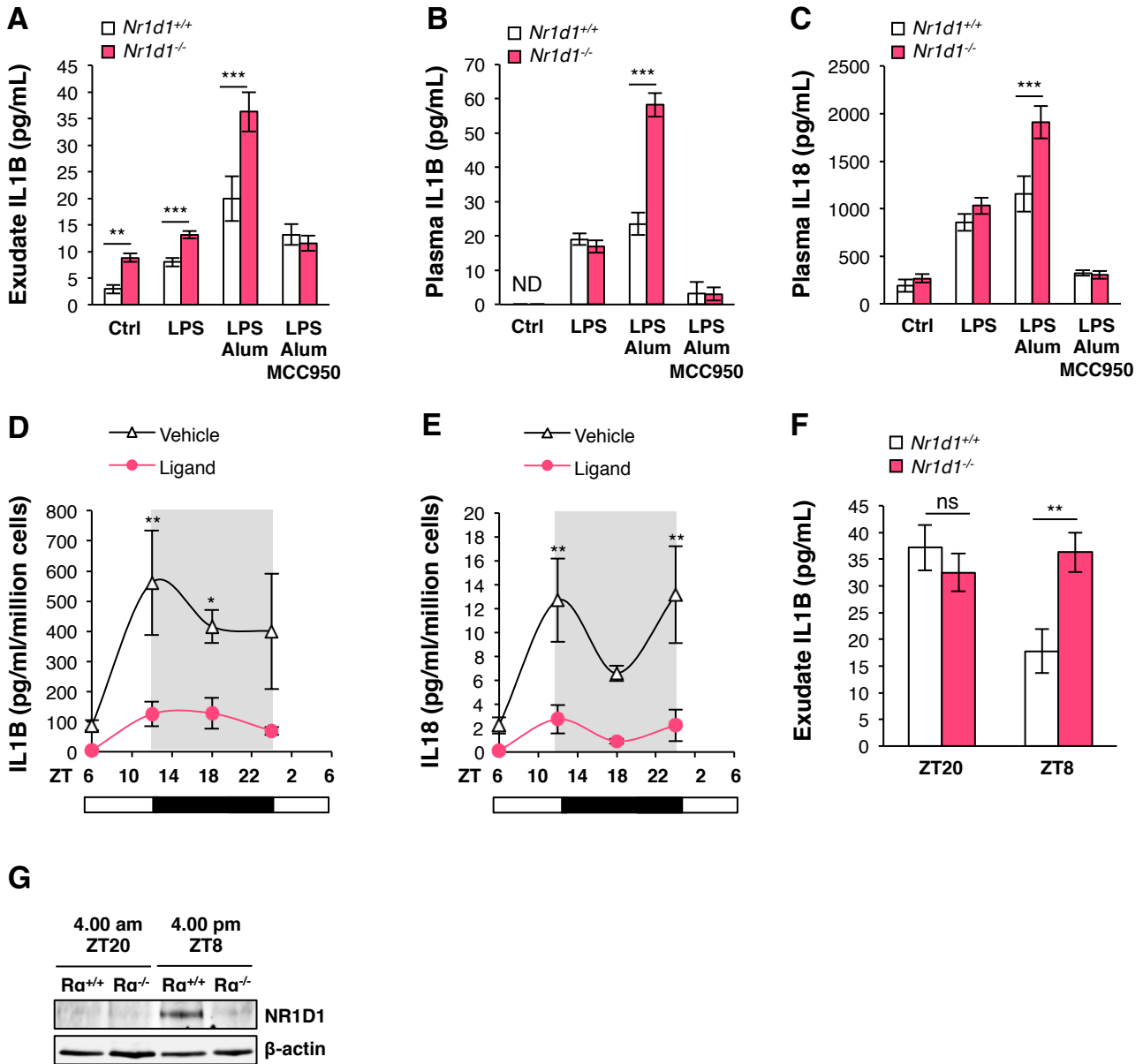
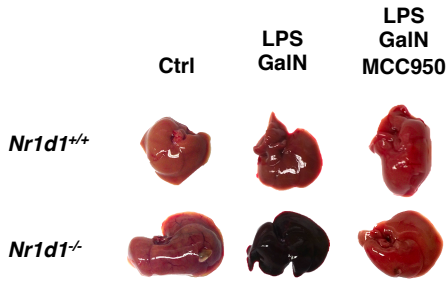


Figure 6: NR1D1 modulates the development of acute innate inflammation through regulation of the NLRP3 inflammasome in a peritonitis model.

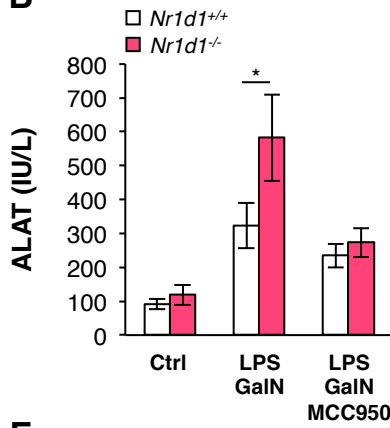
(A) Secreted IL1B from peritoneal lavage of *Nr1d1*^{+/+} or *Nr1d1*^{-/-} mice treated with LPS, LPS + Alum, LPS + Alum + MCC950 or not (Ctrl) at ZT8 (n=6-12). (B) Plasma IL1B and (C) IL18 from *Nr1d1*^{+/+} or *Nr1d1*^{-/-} mice treated as in (A) (n=6-12). (D) Secreted IL1B and (E) IL18 from peritoneal macrophages isolated around the clock from LPS-stimulated mice treated with SR10067 (Ligand) or vehicle (n=10). (F) Secreted IL1B from peritoneal lavage at ZT8 and ZT20 of *Nr1d1*^{+/+} or *Nr1d1*^{-/-} mice treated with LPS + Alum (n=6-12). Data are represented as means ± SEM. *p<0.05, **p<0.01, ***p<0.001 as determined by two-way ANOVA and Bonferroni post-hoc test. (G) NR1D1 protein expression in CD11b⁺ PECs at ZT8 and ZT20 of *Nr1d1*^{+/+} (Ra^{+/+}) or *Nr1d1*^{-/-} (Ra^{-/-}) mice treated with LPS + Alum (n=6-12).

FIGURE 7

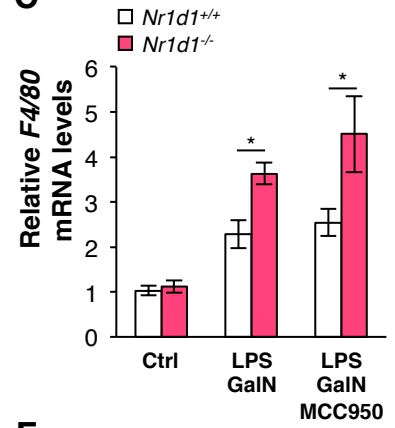
A



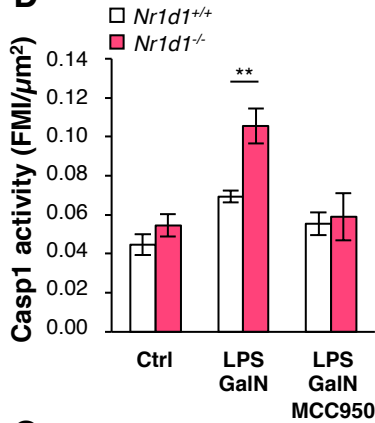
B



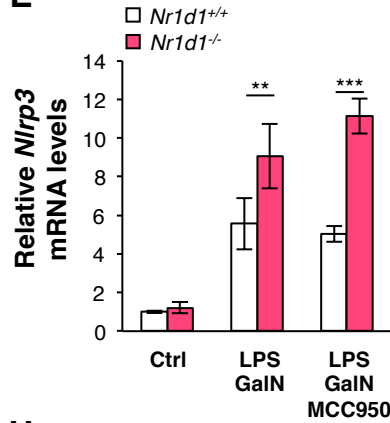
C



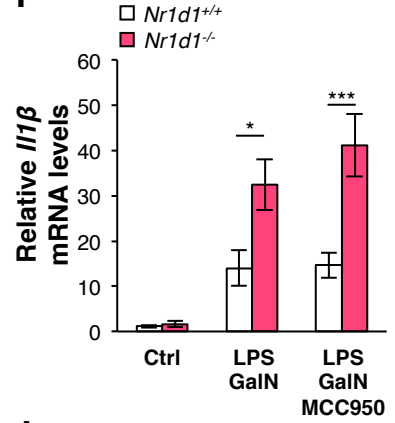
D



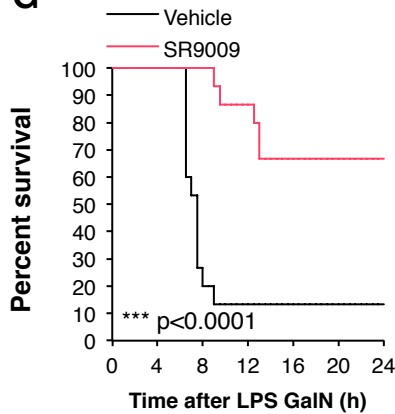
E



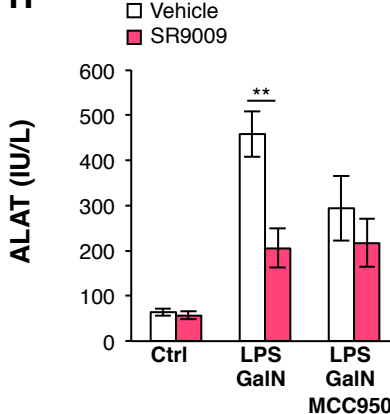
F



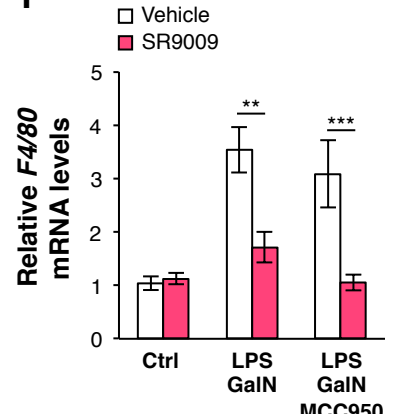
G



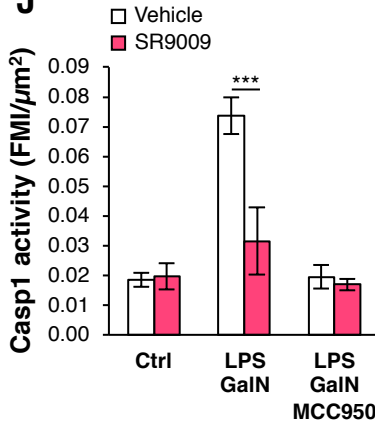
H



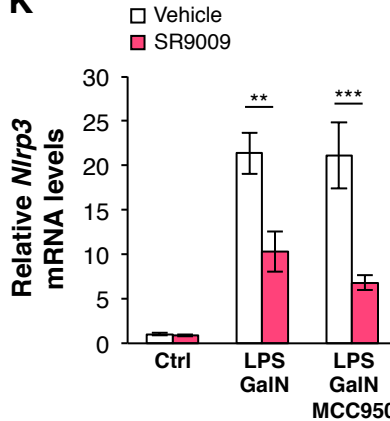
I



J



K



L

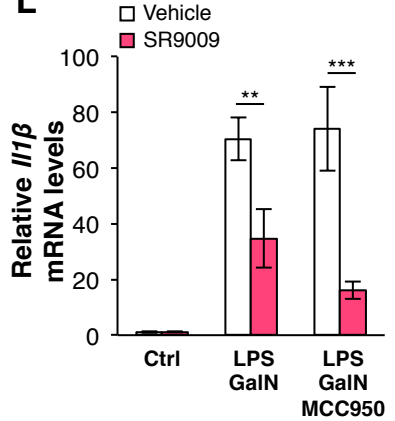


Figure 7: NR1D1 prevents the development of fulminant hepatitis through regulation of the NLRP3 inflammasome.

(A-F) *Nr1d1*^{+/+} or *Nr1d1*^{-/-} mice were pre-treated with MCC950 or Saline and then intraperitoneally injected with LPS plus GaIN or PBS as control (Ctrl). (A) Representative liver appearance, (B) serum ALAT activity, (C) liver *F4/80* mRNA levels, (D) Caspase 1 activity in tissue sections (FMI: Fluorescence Mean Intensity) and (E) *Nlrp3* and (F) *Il1β* mRNA levels in liver from each group as described. Data are represented as means ± SEM (n=5-11). *p<0.05, **p<0.01, ***p<0.001 as determined by two-way ANOVA and Bonferroni post-hoc test. (G-L) C57/Bl6 mice were pre-treated with SR9009 or vehicle and/or MCC950 and then challenged with LPS/GaIN or PBS as control (Ctrl) as indicated. (G) Kaplan-Meier survival curve of mice challenged with LPS/GaIN at ZT2 (n=15 per group). ***p<0.0001 as determined by log rank test. (H) serum ALAT activity, (I) liver *F4/80* mRNA levels, (J) Caspase 1 activity in tissue sections (FMI: Fluorescence Mean Intensity), and (K) *Nlrp3* and (L) *Il1β* mRNA levels in liver from each group as described. Data are represented as means ± SEM (n=5-6) **p<0.01, ***p<0.001 as determined by two-way ANOVA and Bonferroni post-hoc test.

SUPPLEMENTARY FIGURE 1

A

PEC mRNA

		<i>Nr1d1^{+/+}</i>	<i>Nr1d1^{-/-}</i>
<i>Nr1d1</i>	MESOR	1.99 (1.21, 2.77)	NSR
	Amplitude	2.77 (1.6, 3.94)	NSR
	Accrophase	9:12 (7:48, 10:42)	NSR
<i>Nlrp3</i>	MESOR	1.54 (1.34, 1.73)	NSR
	Amplitude	0.946 (0.653, 1.24)	NSR
	Accrophase	20:26 (19:22, 21:30)	NSR
<i>Il1β</i>	MESOR	1.08 (0.64, 1.52)	0.88 (0.41, 1.35)
	Amplitude	0.31 (0, 0.33)	0.52 (0.15, 1.18)
	Accrophase	3:54 (20:31, 11:17)	21:06 (17:10, 2:02)
<i>Il18</i>	MESOR	1.86 (1.77, 1.94)	NSR
	Amplitude	0.71 (0.6, 0.82)	NSR
	Accrophase	23:41 (23:02, 0:20)	NSR

B

PEC ELISA

		<i>Nr1d1^{+/+}</i>	<i>Nr1d1^{-/-}</i>
IL-1b	MESOR	80.8 (65.3, 96.8)	86.6 (69.7, 103)
	Amplitude	34.9 (15.0, 56.6)	47.4 (20.9, 74.1)
	Accrophase	15.1 (13.7, 16.4)	6.85 (5.59, 8.00)
	Period (hrs)	13.93 (11.6, 16.3)	11.92 (10.92, 12.91)
IL18	MESOR	1104 (1027, 1180)	1099 (1019, 1180)
	Amplitude	138.8 (41.1, 247.6)	257.3 (129.9, 384.8)
	Accrophase	14.45 (12.95, 16.5)	18.94 (18.1, 19.8)
	Period (hrs)	12.76 (10.87, 16.5)	11.98 (11.1, 12.8)

C

Synchronised BMDM

		<i>Nr1d1^{+/+}</i>	<i>Nr1d1^{-/-}</i>
<i>Nr1d1</i>	MESOR	0.81 (0.7, 0.92)	NSR
	Amplitude	0.48 (0.32, 0.64)	
	Accrophase	19:58 (18:46, 21:10)	
<i>Nr1d2</i>	MESOR	0.78 (0.71, 0.85)	0.9 (0.82, 0.98)
	Amplitude	0.27 (0.16, 0.37)	0.27 (0.15, 0.39)
	Accrophase	20:47 (19:17, 22:16)	21:11 (19:32, 22:51)
<i>Nlrp3</i>	MESOR	1.49 (1.26, 1.70)	2.18 (2.05, 2.32)
	Amplitude	0.21 (-0.02, 0.40)	0.3 (0.1, 0.51)
	Accrophase	8:30 (4:44, 13:12)	5:58 (3:44, 8:13)
<i>Arntl</i>	MESOR	1.1 (1.07, 1.21)	1.4 (1.32, 1.48)
	Amplitude	0.45 (0.34, 0.54)	0.1916 (0.09, 0.30)
	Accrophase	6:58 (6:07, 7:52)	12:08 (9:51, 14:35)
<i>Il18</i>	MESOR	0.88 (0.77, 0.99)	NSR
	Amplitude	0.26 (0.09, 0.43)	
	Accrophase	6:55 (4:38, 9:21)	

D

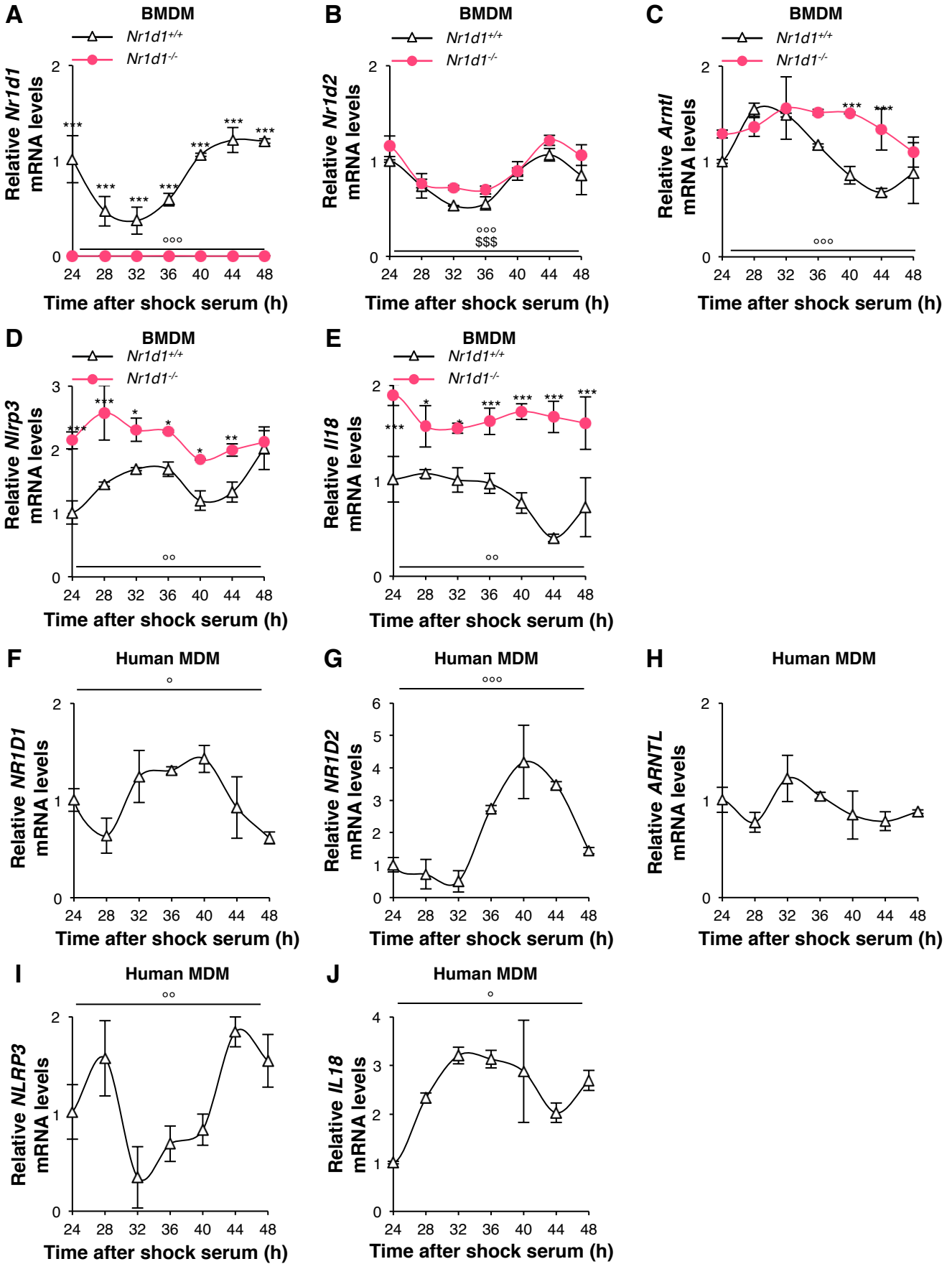
Synchronised human MDM

			R ² for model
<i>NR1D1</i>	MESOR	1.07 (0.86, 1.28)	0,6393
	Amplitude	0.36 (0.08, 0.63)	
	Accrophase	1:29 (23:15, 4:43)	
<i>NR1D2</i>	MESOR	2.11 (1.68, 2.53)	0,883
	Amplitude	1.97 (1.35, 2.59)	
	Accrophase	16:42 (15:36, 17:47)	
<i>NLRP3</i>	MESOR	1.02 (0.79, 1.25)	0,5176
	Amplitude	0.53 (-0.09, 1.15)	
	Accrophase	22:22 (17:32, 3:13)	
<i>ARNTL</i>	MESOR	0.95 (0.86, 1.04)	0,298
	Amplitude	0.14 (0, 0.27)	
	Accrophase	8:41 (4:57, 13:58)	
<i>IL18</i>	MESOR	2.61 (2.24, 2.99)	0,3459
	Amplitude	0.65 (0.19, 1.13)	
	Accrophase	10:55 (7:43, 14:42)	

Supplementary Figure 1: Cosinor analysis of mRNA and cytokine oscillation.

(A) CD11b⁺ PEC mRNA (B) CD11b⁺ PEC ELISA (C) synchronised BMDM and (D) synchronised human MDM.

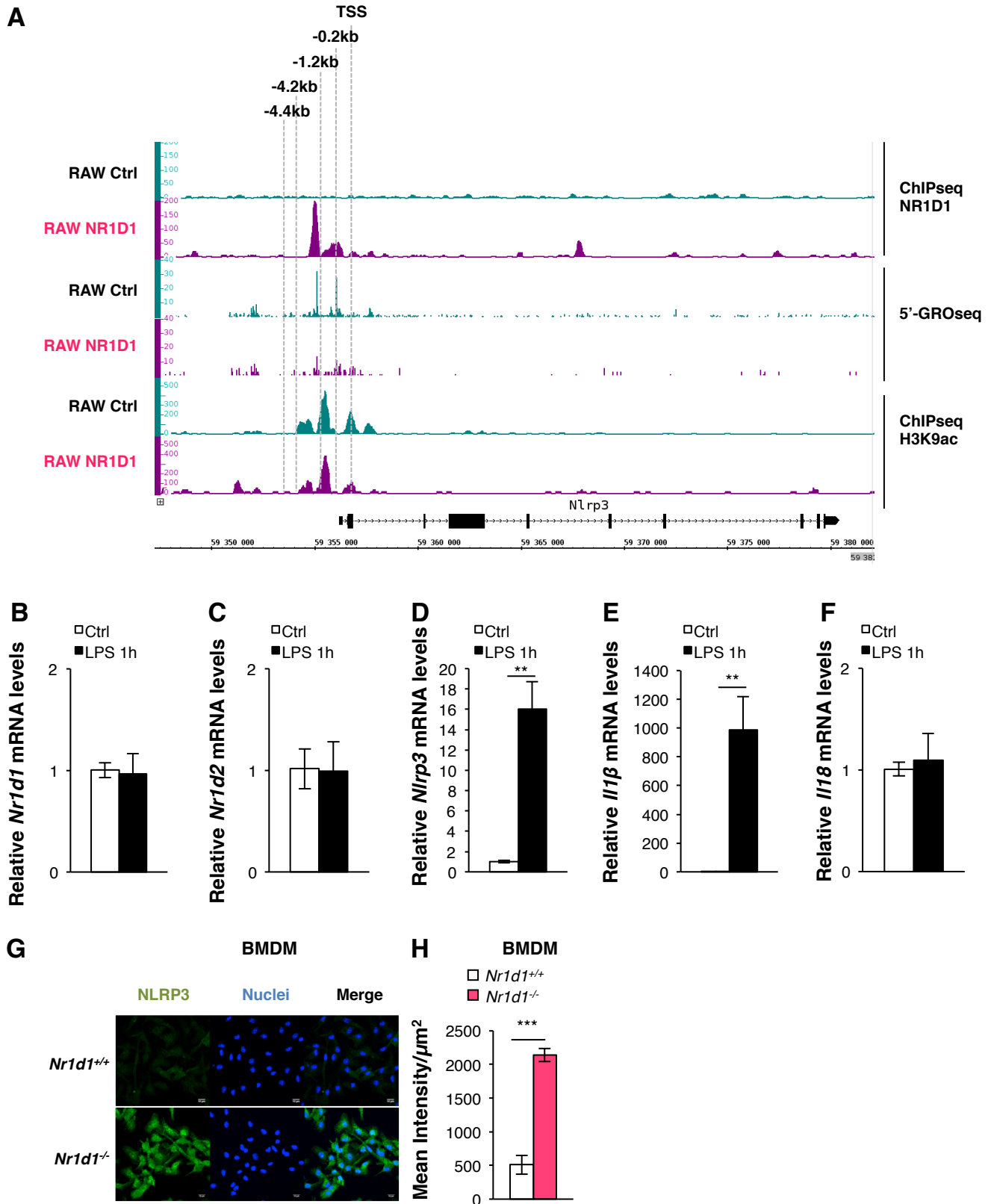
SUPPLEMENTARY FIGURE 2



Supplementary Figure 2: Gene expression of the NLRP3 inflammasome pathway displays circadian oscillations in synchronized mouse BMDMs and human MDMs.

(A) *Nr1d1*, (B) *Nr1d2*, (C) *Arntl*, (D) *Nlrp3* and (E) *Il18* mRNA levels in BMDMs from *Nr1d1^{+/+}* or *Nr1d1^{-/-}* mice that were synchronized in vitro by serum shock. Data are means \pm SD (n=3). *p<0.05, **p<0.01, ***p<0.001 as determined by two-way ANOVA and Bonferroni post-hoc test to compare *Nr1d1^{+/+}* or *Nr1d1^{-/-}* mice. °p<0.01, °°p<0.001 as determined by one-way ANOVA to assess variation over time in *Nr1d1^{+/+}* cells, and \$\$\$p<0.001 as determined by one-way ANOVA to assess variation over time in *Nr1d1^{-/-}* cells. (F) *NR1D1*, (G) *NR1D2*, (H) *ARNTL*, (I) *NLRP3* and (J) *IL18* mRNA levels in human MDMs that were synchronized by serum shock. Data are means \pm SD (n=3). °p<0.05, °°p<0.01, °°°p<0.001 as determined by one-way ANOVA to assess variation over time in human MDMs.

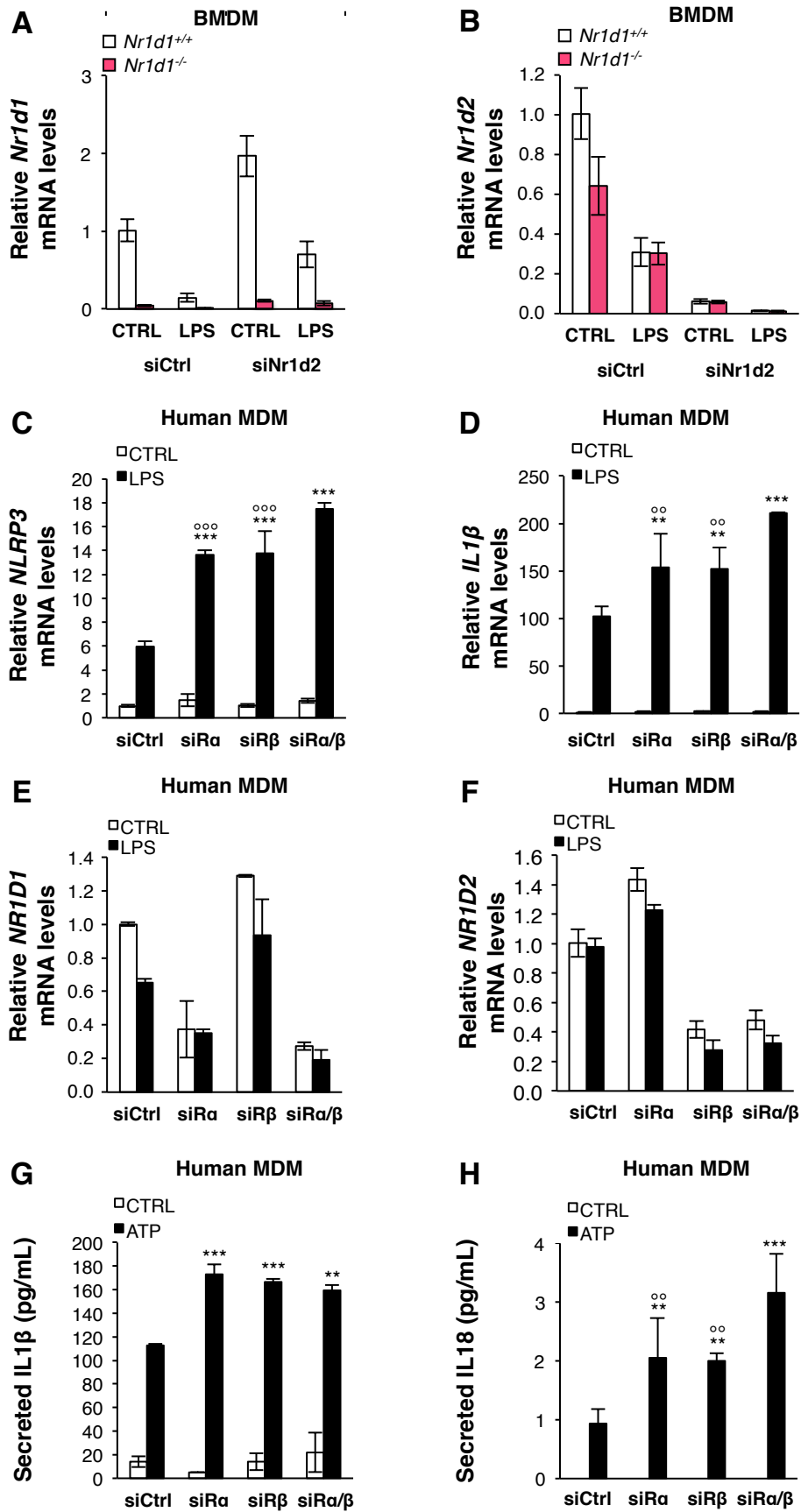
SUPPLEMENTARY FIGURE 3



Supplementary Figure 3: NR1D1 regulates *Nlrp3* expression.

(A) Analysis of ChIPseq and 5'Gro-seq data from²³ showing that NR1D1 binds to and represses transcription from the *Nlrp3* promoter in *Nr1d1* overexpressing RAW264.7 macrophages. (B) *Nr1d1*, (C) *Nr1d2*, (D) *Nlrp3*, (E) *Il1b* and (F) *Il18* mRNA levels in BMDMs treated with LPS during 1 hour (LPS 1h) or not (Ctrl) (n=3). **p<0.001 as determined by unpaired t-test. (G, H) Quantification of NLRP3 protein expression from NLRP3 immunofluorescence in LPS-primed BMDMs from *Nr1d1*^{+/+} or *Nr1d1*^{-/-} mice (n=3). Data are mean values \pm SD (at least 150 cells per slide). ***p<0.001 as determined by unpaired two-tailed t-test.

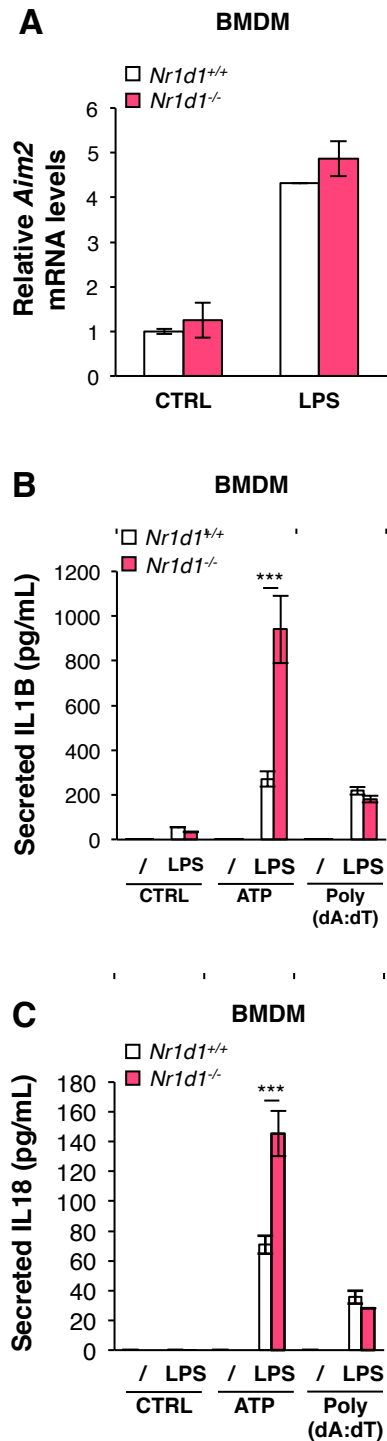
SUPPLEMENTARY FIGURE 4



Supplementary Figure 4: Both NR1D1 and NR1D2 regulate the NLRP3 inflammasome pathway in human MDMs.

(A) *Nr1d1* and (B) *Nr1d2* mRNA levels in LPS-primed (LPS) or not (CTRL) BMDMs from *Nr1d1*^{+/+} or *Nr1d1*^{-/-} mice transfected with siRNA against *Nr1d2* (siNr1d2) or a scrambled siRNA (siCtrl). (C) *NLRP3*, (D) *IL1 β* , (E) *REV-ERBa*, (F) *NR1D2* mRNA levels in LPS-primed (LPS) or not (CTRL) human MDMs and (G) *IL1 β* and (H) *IL18* secretion in LPS-primed and ATP-activated (ATP) or not (CTRL) human MDMs transfected with a siRNA against *Nr1d1* (siRa) and/or *Nr1d2* (siR β) or a scrambled siRNA (siCtrl). Data are mean values \pm SD (n=3). Vs siCtrl **p<0.01, ***p<0.001 as determined by two-way ANOVA followed by a Bonferroni post-hoc test. Vs siRNA *Nr1d1* siRNA *Nr1d2* ^{oo}p<0.01, ^{ooo}p<0.001 as determined by two-way ANOVA followed by a Bonferroni post-hoc test.

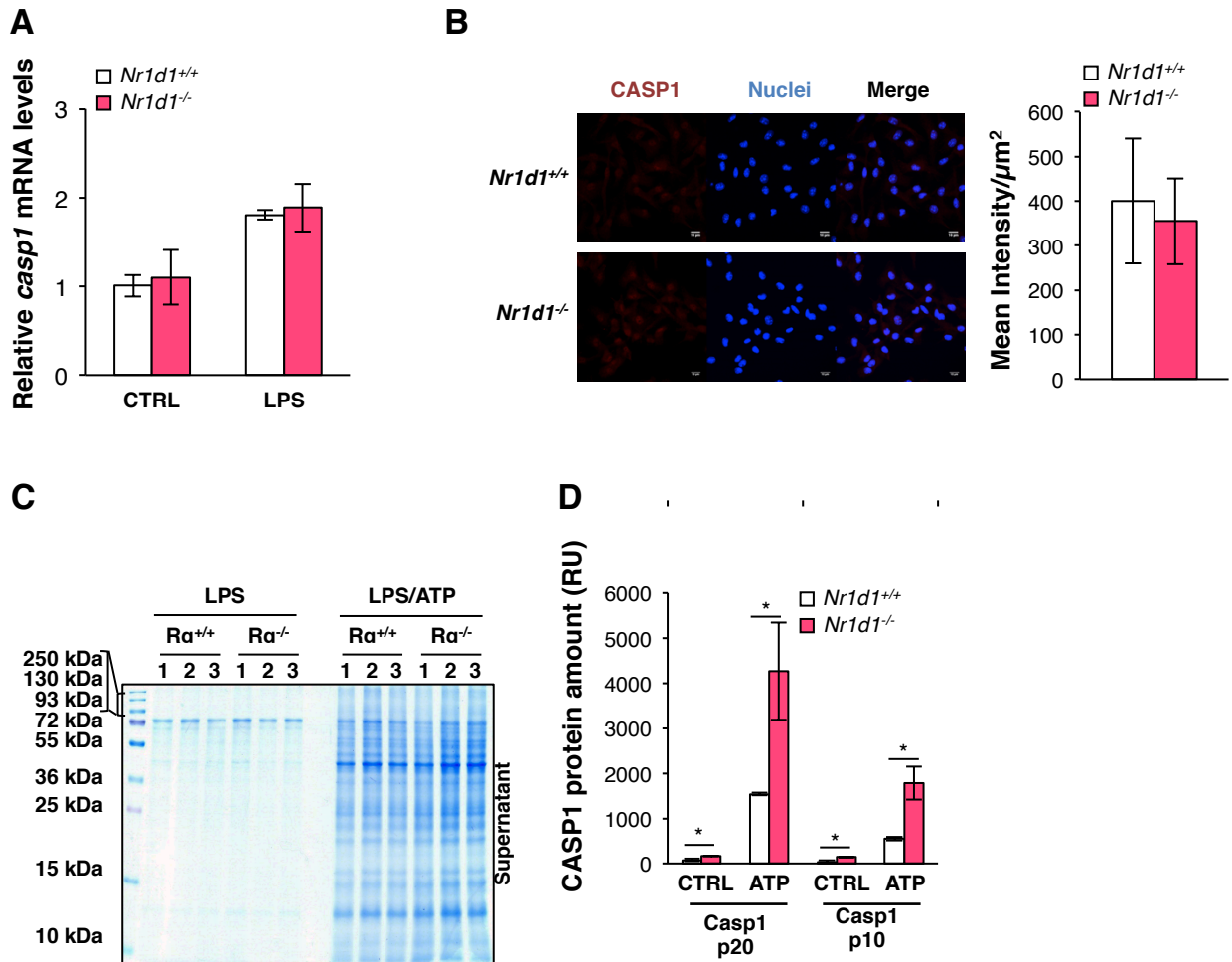
SUPPLEMENTARY FIGURE 5



Supplementary Figure 5: NR1D1 does not regulate the AIM2 inflammasome.

(A) *Aim2* mRNA levels in LPS-primed (LPS) or not (CTRL) BMDMs from *Nr1d1*^{+/+} or *Nr1d1*^{-/-} mice. (B) IL1B and (C) IL18 secretion in LPS-primed (LPS) or not (/) and activated with ATP (ATP) or Poly(dA:dT) BMDMs from *Nr1d1*^{+/+} or *Nr1d1*^{-/-} mice. Data are mean values \pm SD (n=3). ***p<0.001 as determined by two-way ANOVA and Bonferroni post-hoc test.

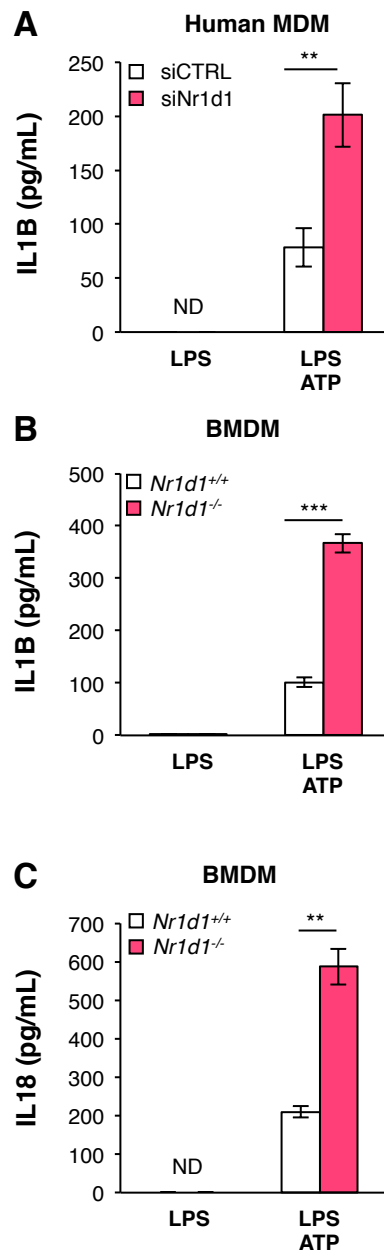
SUPPLEMENTARY FIGURE 6



Supplementary Figure 6: Nr1d1 deficiency leads to increased Caspase-1 maturation, but not expression, in primary macrophages.

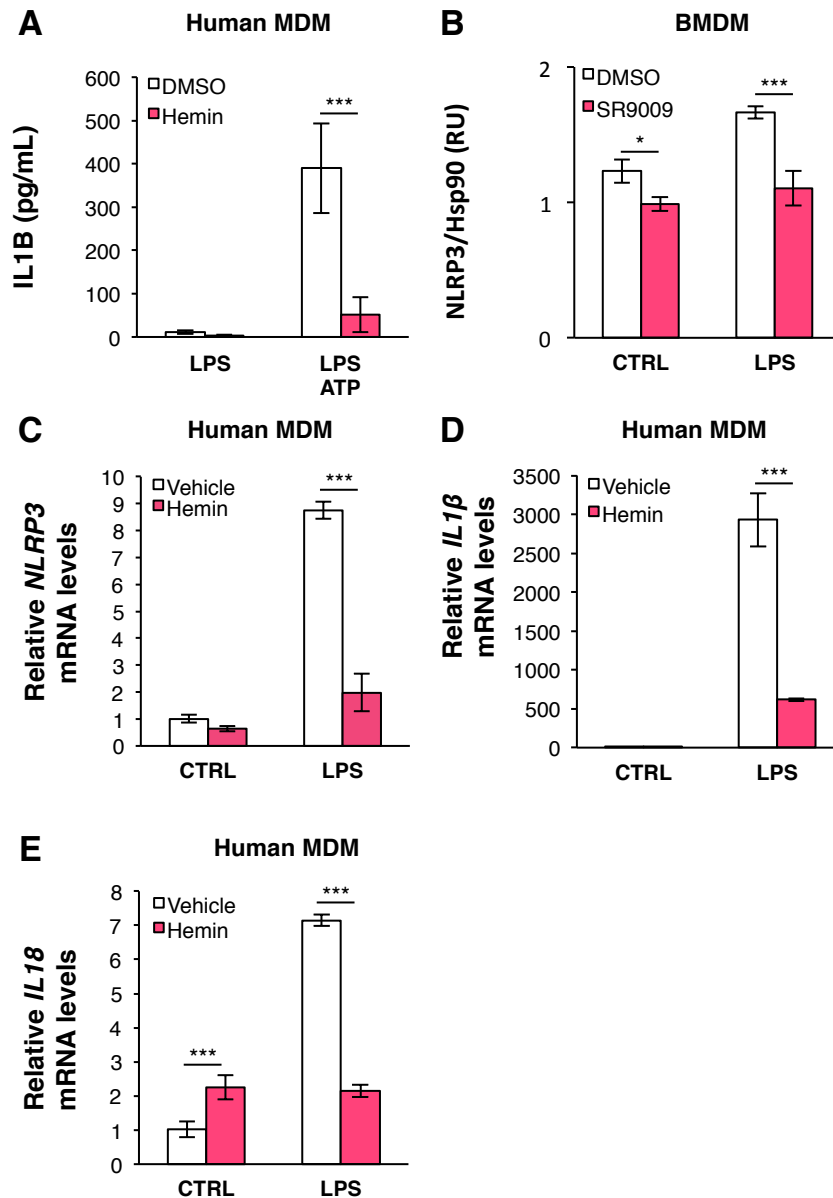
(A-B) Caspase-1 (CASP1) mRNA (A) and protein (B) levels in control (CTRL) or LPS-primed (LPS) BMDMs from *Nr1d1^{+/+}* or *Nr1d1^{-/-}* mice (n=3). Immunofluorescence quantification on at least 150 cells per slide. (C) Total proteins were visualized in the acrylamide gel after a Coomassie blue staining as a loading control for Figure 3A in BMDM isolated from *Nr1d1^{+/+}* (*Ra^{+/+}*) and *Nr1d1^{-/-}* (*Ra^{-/-}*) mice. (D) Western blot quantification of secreted mature Caspase-1 p20 and p10 protein fragments from *Nr1d1^{+/+}* or *Nr1d1^{-/-}* mice BMDMs treated with LPS (CTRL) or with LPS and ATP (ATP). Data are means \pm SD (n=3). *p<0.05, as determined by two-way ANOVA and Bonferroni post-hoc test.

SUPPLEMENTARY FIGURE 7



Supplementary Figure 7: *Nr1d1* deficiency increases IL1B and IL18 secretion in primary macrophages. (A) IL1B secretion in LPS-primed (LPS) and ATP-activated (LPS ATP) human MDMs in which *Nr1d1* has been silenced (siNr1d1). (B) IL1B and (C) IL18 secretion in LPS-primed (LPS) and ATP-activated (LPS ATP) BMDMs from *Nr1d1*^{+/+} or *Nr1d1*^{-/-} mice. Data are means \pm SD (n=3). **p<0.01, ***p<0.001 as determined by two-way ANOVA and Bonferroni post-hoc test.

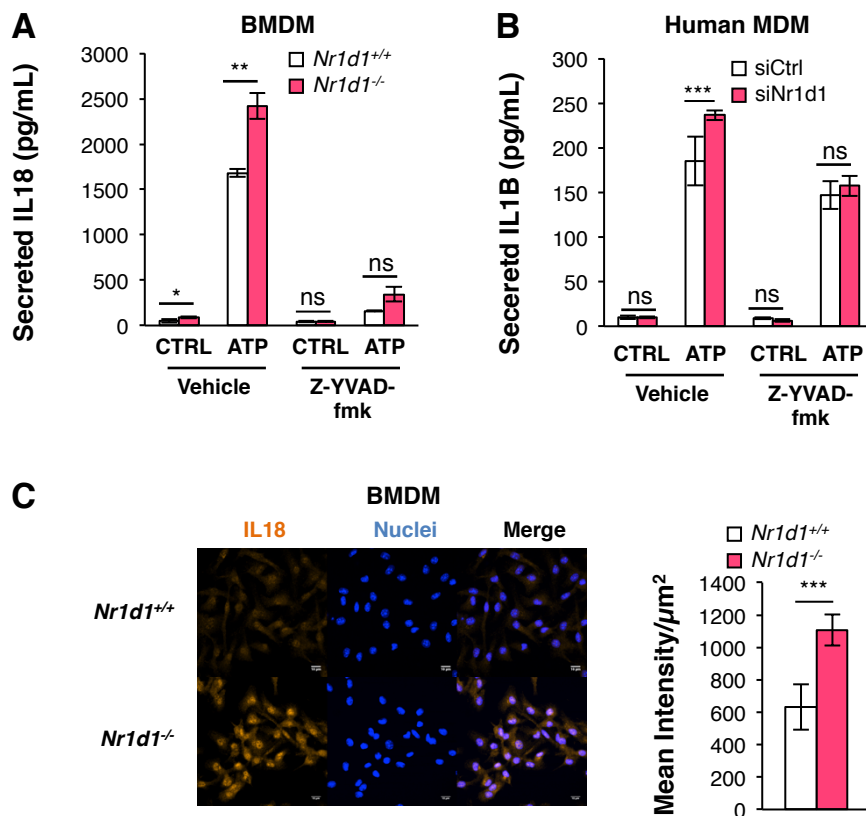
SUPPLEMENTARY FIGURE 8



Supplementary Figure 8: NR1D1 pharmacological activation downregulates the NLRP3 inflammasome pathway.

(A) IL1B secretion in LPS-primed (LPS) and ATP-activated (LPS+ATP) human MDMs treated with Hemin or not (Vehicle). (B) NLRP3 protein quantification of Fig. 5B in LPS-primed (LPS) or not (CTRL) BMDMs treated with SR9009 or DMSO as control. (C) *NLRP3* (D) *IL1β* and (E) *IL18* mRNA levels in LPS-primed (LPS) or not (CTRL) human MDMs treated with Hemin or not (Vehicle). Data are means ± SD (n=3). ***p<0.001 as determined by two-way ANOVA and Bonferroni post-hoc test.

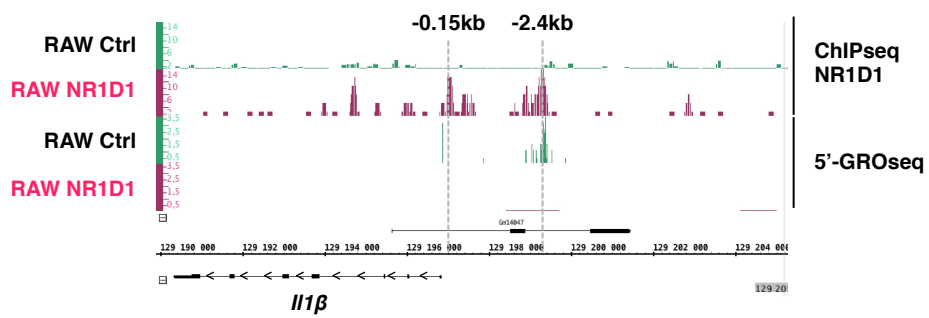
SUPPLEMENTARY FIGURE 9



Supplementary Figure 9: NR1D1 controls IL1B and IL18 secretion in a Caspase-1-dependent manner.

(A) IL18 secretion in LPS-primed (CTRL) and ATP-activated (ATP) BMDMs from *Nr1d1*^{+/+} or *Nr1d1*^{-/-} mice. (B) IL1B secretion in LPS-primed (CTRL) and ATP-activated (ATP) in human MDMs in which *Nr1d1* has been silenced (siNr1d1). These samples were treated with a caspase 1 inhibitor Z-YVAD-fmk or not (Vehicle). Data are means \pm SD (n=3). **p<0.01, ***p<0.001 as determined by two-way ANOVA and Bonferroni post-hoc test. (C) Intracellular IL18 protein in LPS-primed BMDMs from *Nr1d1*^{+/+} or *Nr1d1*^{-/-} mice (n=3). Quantification of intracellular IL18 from 150 cells/slide. Data are means \pm SD. ***p<0.001 as determined by unpaired two-tailed student t-test.

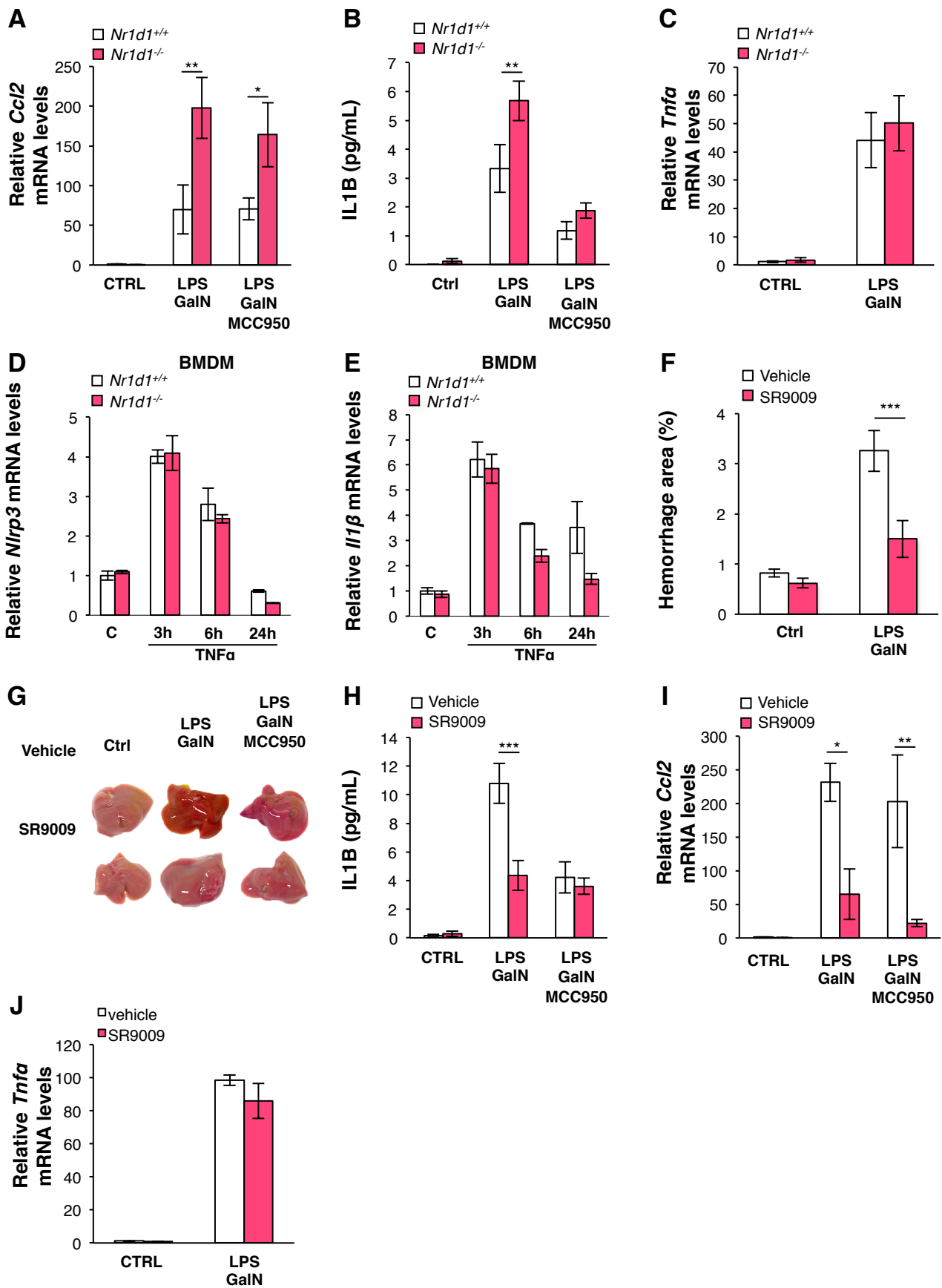
SUPPLEMENTARY FIGURE 10



Supplementary Figure 10: NR1D1 binds to the *II1β* promoter and inhibits de novo transcription.

Analysis of ChIPseq and 5'Gro-seq data from Lam et al.²³ showing that NR1D1 binds to and represses transcription from the *II1β* promoter in *Nr1d1*-overexpressing RAW264.7 macrophages.

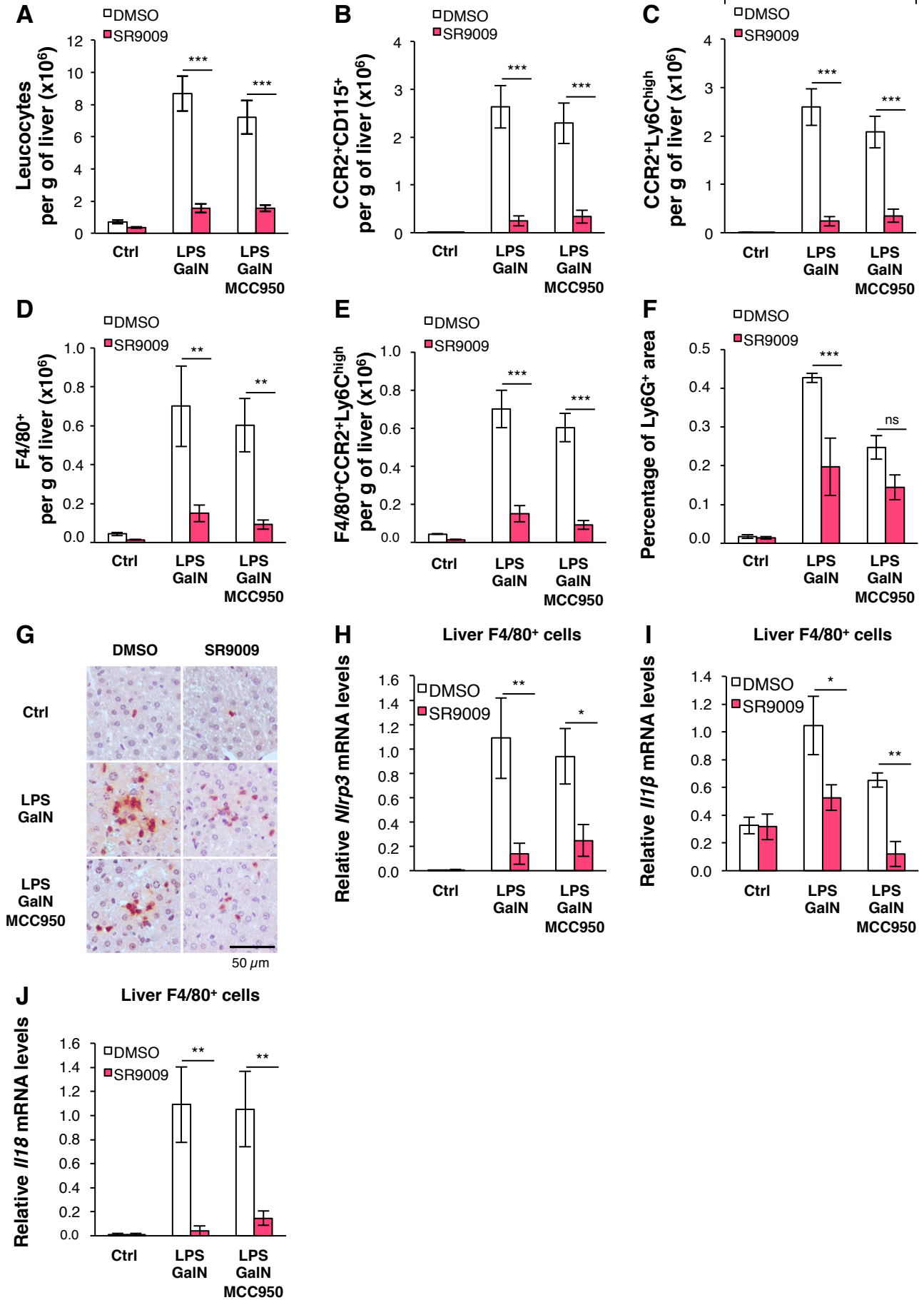
SUPPLEMENTARY FIGURE 11



Supplementary Figure 11: NR1D1 prevents the development of fulminant hepatitis in a NLRP3-dependent manner.

(A) Liver *Ccl2* and (C) *Tnfa* mRNA levels, and (B) secreted IL1B in blood sampled from $Nr1d1^{+/+}$ and $Nr1d1^{-/-}$ mice pre-treated with MCC950 or saline and then injected with LPS/GalN. Data are means \pm SEM (n=5-6). *p<0.05, **p<0.01 as determined by two-way ANOVA and Bonferroni post-hoc test. (D-E) *Nlrp3* (D) and *Il1β* mRNA (E) levels in BMDMs from $Nr1d1^{+/+}$ and $Nr1d1^{-/-}$ mice primed with TNF α during 3, 6 or 24 hours. Data are means \pm SD (n=3). (F) Hemorrhage area in liver, (G) Representative liver appearance, (H) Secreted IL1B in blood samples, and (I) Liver *Ccl2* and (J) *Tnfa* mRNA levels from mice pre-treated with SR9009 or Vehicle and MCC950 or Saline, and then intraperitoneally challenged with LPS plus D-Galactosamine (GalN). Data are means \pm SEM (n=5-6). Data are means \pm SEM. *p<0.05, **p<0.01, ***p<0.001 as determined by two-way ANOVA and Bonferroni post-hoc test.

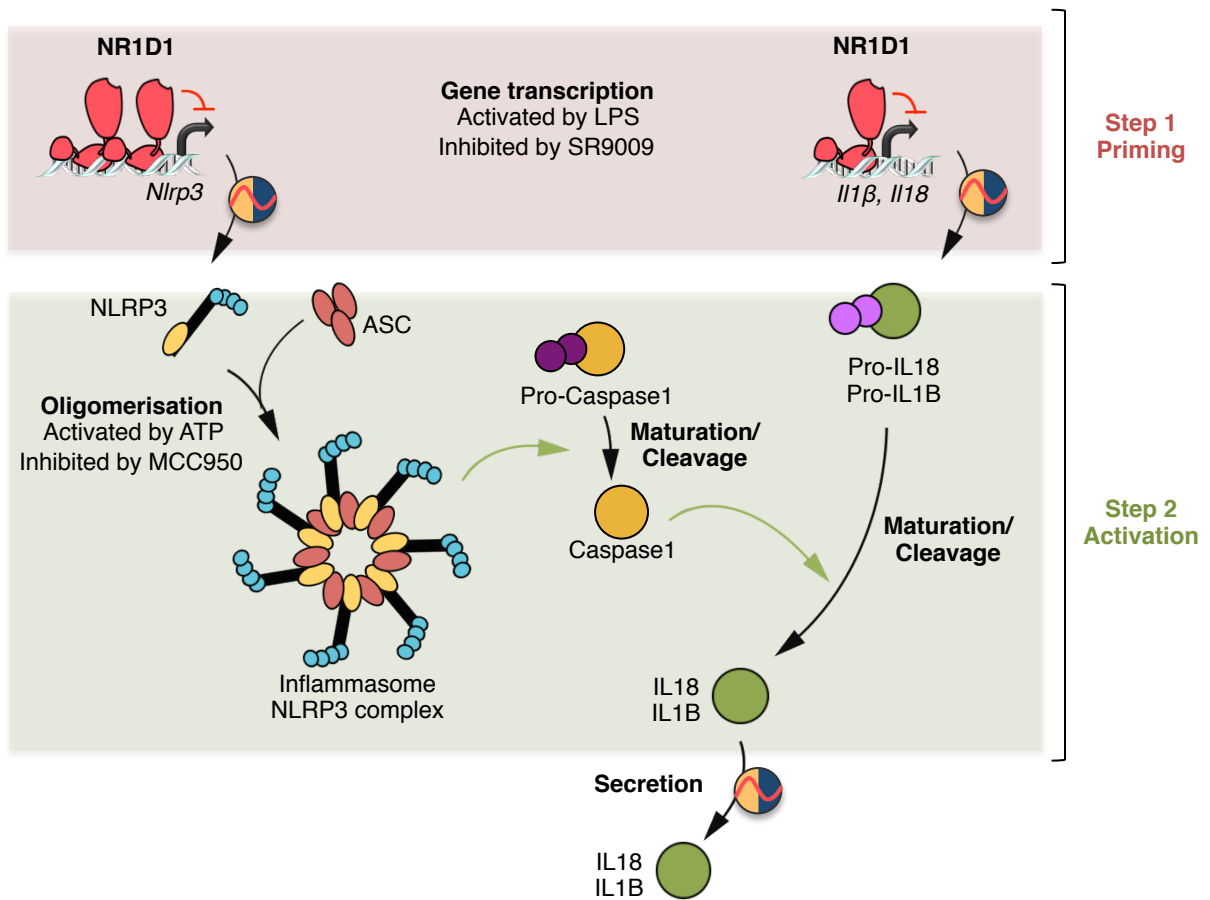
SUPPLEMENTARY FIGURE 12



Supplementary Figure 12: NR1D1 pharmacological activation reduces leukocytes recruitment to the liver in fulminant hepatitis.

C57/Bl6 mice were pre-treated with SR9009/DMSO and/or MCC950/Vehicle and then challenged with LPS/GaIN or PBS as control (Ctrl). Immune cells were isolated on a Percoll gradient, counted and analyzed by Flow cytometry. (A) Leucocytes, (B) monocytes (CCR2⁺CD115⁺), (C) infiltrating monocytes (CCR2⁺Ly6C^{high}), (D) macrophages (F4/80⁺) and (E) recruited macrophages (F4/80⁺CCR2⁺Ly6C^{high}) number per g of liver. (F) Quantification and (G) Representative neutrophil staining (Ly6G⁺) on liver sections. Data are means \pm SEM (n=6). **p<0.01, ***p<0.001 as determined by two-way ANOVA and Bonferroni post-hoc test. (H) *Nlrp3* (I) *Il1 β* and (J) *Il18* mRNA levels in F4/80⁺ cells. Data are means \pm SEM (n=6). *p<0.05, **p<0.01 as determined by two-way ANOVA and Bonferroni post-hoc test.

SUPPLEMENTARY FIGURE 13



Supplementary Figure 13: Scheme depicting how NR1D1 regulates the NLRP3 inflammasome pathway.